POLITECNICO DI TORINO
Repository ISTITUZIONALE

Raman and Attenuated Total Reflectance Infrared RRUFF Spectra: some cases of deconvolution with q-Gaussians and q-BWF functions

Original
Raman and Attenuated Total Reflectance Infrared RRUFF Spectra: some cases of deconvolution with q-Gaussians and q-BWF functions / Sparavigna, Amelia Carolina. - ELETTRONICO. - (2024). [10.5281/zenodo.14220559]

Availability:
This version is available at: 11583/2994781 since: 2024-11-26T08:02:34Z

Publisher:
Zenodo

Published
DOI:10.5281/zenodo.14220559

Terms of use:

This article is made available under terms and conditions as specified in the corresponding bibliographic description in the repository

Publisher copyright

(Article begins on next page)

08 May 2026

Raman and Attenuated Total Reflectance Infrared RRUFF Spectra: some cases of deconvolution with q-Gaussians and q-BWF functions

Amelia Carolina Sparavigna

Department of Applied Science and Technology, Polytechnic University of Turin, Italy

Abstract: RRUFF database is proposing Raman and Attenuated Total Reflectance (ATR) Infrared spectra of several minerals. Here we consider some cases, comparing Raman and ATR bands, as determined by the deconvolution of RRUFF spectra, with data from literature. The examples of deconvolutions, obtained by means of q-Gaussian and q-BWF (Breit-Wigner-Fano) functions, are regarding azurite and malachite, siderite and rhodochrosite. A detailed discussion is also given of the ATR infrared spectroscopy techniques that have been proposed, independently, in 1959 by Jacob Fahrenfort, Koninklijke Shell Laboratorium, Amsterdam, and in 1960 by Nicolas James Harrick, Philips Laboratories, New York.

Keywords: Raman spectroscopy, ATR Infrared spectroscopy, q-Gaussian functions, q-BWF functions.

Torino, October 20, 2024, Submitted SSRN:

Introduction

In several previous studies, we have considered the Raman and the ATR (Attenuated Total Reflectance) spectra of several minerals, available from the RRUFF database, and the related spectral deconvolutions obtained by means of q-Gaussian and q-BWF (Breit-Wigner-Fano) functions (see definitions in Appendix A). In particular, we considered the detection of crystallization water in the cases of minerals of vivianite and natrolite groups, using the Raman spectra deconvoluted into q-Gaussian functions. Water was also investigated in gypsum with Raman and ATR spectra. In analyses of barite-group and carbonate minerals, we found the ATR bands appearing asymmetrical (Kendix, 2009), and therefore, for their deconvolution, we used the asymmetric q-BWF functions. Here we analyze further cases of Raman and ATR-infrared RRUFF spectra. A detailed discussion is also given of the ATR spectroscopy techniques that have been proposed, independently, in 1959 by Jacob Fahrenfort, Koninklijke Shell Laboratorium, Amsterdam, and in 1960 by Nicolas James Harrick, Philips Laboratories, New York.

The ATR spectra provided by RRUFF have been collected at the California Institute of Technology, http://minerals.gps.caltech.edu/ (Lafuente et al., 2015). "Similarly to Raman spectroscopy, the infrared spectrum can provide additional information … The two techniques are complementary because while Raman scattering requires a change in polarizability with vibration, infrared requires a change in dipole moment. Therefore, in molecules with different elements of symmetry, certain bands may be infrared active, Raman active, both or neither" (Lafuente et al., 2015). Powder samples were used for collecting RRUFF ATR-infrared spectra in Caltech George Rossman's laboratory. Instrumentation is a SensIR Durascope on a Nicolet Magna 860 FTIR. Before showing examples of deconvolutions of RRUFF spectra, let us remember some general facts regarding Raman and ATR spectroscopies.

RRUFF Raman spectroscopy

In Lafuente et al., we can find details about the RRUFF Raman spectroscopy. "During the analysis, the transfer of energy of the incident photons (gain or loss) results in a spectrum of energy shifts characteristic of the chemistry and structure of the compound, and therefore, may provide a *fingerprint* that can be used in the

identification of most minerals" (Lafuente et al., 2015). The first use of the term 'fingerprint' for Raman spectroscopy, to the best of my knowledge, is in an article published in 1947, about the Raman spectra of hydrocarbons (Fenske et al., 1947). "The basis for applying Raman spectroscopy to hydrocarbon analysis is dependent upon the fact that when a beam of a monochromatic exciting light passes through a transparent medium some of the light is absorbed and may be re-emitted. If this re-emitted light is examined by means of a spectrograph, very weak spectral lines or bands will appear on either side of the line of the exciting light. These weak lines, which are called Raman lines, are characteristic of the substance illuminated and are therefore a "fingerprint" of that substance" (Fenske et al., 1947). From that time on, the points of identification, such as positions of peaks, shoulders and valleys are considered to constitute the characteristic spectral pattern which is defined as the *Raman fingerprint* of a given material.

Fingerprint allows the material classification, "without any preliminary information about composition and structural origin of the individual features" (D'Ippolito, et al., 2015). In this manner, the Raman spectroscopy is used for routine investigations "in materials science, cultural heritage, mineralogy, geology, and gemology and plays an important role also in astromineralogy" (D'Ippolito et al. and references therein; the characterization of materials on Mars is also mentioned). We have a fingerprint matching when the peak positions are almost the same.

"The power of the RRUFF project lies in its capability to aid in mineral identification and characterization. Records of well-characterized minerals can be used as a reliable Raman reference, and the ancillary software, including CrystalSleuth, XtalDraw, and XPOW, provides visualization and manipulation of data" (Lafuente et al., 2015). The database can be used for further projects; for instance, "RRUFF database and CrystalSleuth are used by Kuehn to study the application of Raman spectroscopy for the identification of gemstones" (Lafuente et al., 2015). For a simple and rapid approach to spectral data processing for identification of minerals, it is possible to use the first derivative of the spectrum, that is, the "first derivative spectrum" (Mosier-Boss et al., 1995). For spectral comparisons, this processing may be used standalone, that is without any further fitting procedure regarding the deconvolution of the spectrum in components. However, also in the case of a first derivative spectrum approach, the method is not trivial, as discussed in SSRN.

In general, in the RRUFF database we can find spectra obtained from unoriented samples excited with 532 (green) and 785/780 (red) nm lasers. In RRUFF we can find high-resolution scans, usually given from 70–1400 cm^{-1}, and low-resolution broad scans, usually given from 70–4000 or 70–6500 cm^{-1}. Scans "are collected with the 532 and 785/780 nm lasers from *exactly the same spot* in the sample and until the signal to noise ratio is optimal" (Lafuente et al., 2015). "The low-resolution wide scans are performed with both 532 and 785 nm lasers in order to record other Raman peaks, such as the *O-H stretching modes*, and other spectral artifacts. With our [RRUFF] instrument, only the spectra collected with the 532 nm laser reveal the presence of O-H bands that are often located in the 2700–3700 cm^{-1} region … The sensitivity of the silicon detector in the 785 nm laser is quite poor at higher wavenumbers which makes it useless for the detection of the O-H modes" (Lafuente et al., 2015). In the database we can find raw data, and spectra processed by means of the CrystalSleuth, for instance, to correct the baseline. "The intensities of certain Raman peaks of a mineral may vary appreciably as a function of sample orientation, … Thus, in certain cases, especially for rock-forming minerals, Raman spectra collected in additional different orientations with respect to the polarization direction of the incident laser are collected. The analyses are conducted with an IRIS Raman instrument built by Alex Goncharov and Victor Struzhkin of the Geophysical Laboratory at the Carnegie Institution of Washington" (Lafuente et al., 2015).

About ATR spectroscopy, it is better to add some notes about this spectroscopy.

The principle of ATR

An ATR technique was proposed as based on the "attenuated total reflection, a new principle for the production of useful infra-red reflection spectra of organic compounds" by Jacob Fahrenfort, Koninklijke Shell Laboratorium, Amsterdam, at the Meeting of the European Molecular Spectroscopy Group, Bologna, 1959,

(article published in Spectrochimica Acta, 1961). The concept of ATR method, "as developed by Fahrenfort" allows to obtain "intense infra-red spectra from samples which were difficult or not amenable to examination by normal transmission techniques" (Baxter & Puttnam, 1965). "The radiation incident on the interface between the analyzing crystal and the sample, at angles of incidence greater than the critical angle, will be totally reflected at those wavelengths where the sample shows no absorption. However, at those wavelengths where the sample absorbs, part of the incident radiation will be absorbed, causing a decrease, that is an attenuation, in the intensity of the reflected radiation. This will produce a spectrum which strongly resembles the transmission spectrum, although the shape of the bands will be different" (Baxter & Puttnam, 1965, mentioning Fahrenfort & Vissen, 1962).

Let us report the summary of the contribution by Jacob Fahrenfort, at the Meeting in Bologna,1959. "Conventional infrared reflection spectra of organic compounds are generally characterized by their lack of detail and consequently yield very little information. At the low absolute level of the absorption index κ prevailing in these materials in the infrared region, the intensity of reflection is hardly affected even by fairly large relative changes in the value of κ. This causes the reflection spectra to show considerably less contrast between regions of transparency and absorption than do absorption spectra. A greater improvement of this contrast is obtained if a *new method based on the principle of attenuated total reflection* is used. Rather than the plain boundary of the sample, the interface between the sample and a transparent medium with a high refractive index, like KRS 5 or AgCl, is taken as the reflecting surface. Under these conditions the relative refractive index at the interface becomes smaller than unity. Radiation incident on the interface at an angle somewhat larger than the critical angle will now be totally reflected, but only in those wave-length regions where the second medium is non absorbing (κ=0). In the wave-length region with $\kappa \neq 0$, reflection will not be total any more, and accordingly an infrared reflection spectrum of high contrast and intensity may be obtained, which strongly resemble a transmission spectrum. These spectra may, after calibration, be used as such for quantitative purposes. They may also, however, by application of the Kramers-Kronig relations, be converted into spectra of the optical constants n and κ, and hence into the absorption spectra. Some examples of spectra obtained with this method will be given." (Fahrenfort, 1959). In Fahrenfort, 1961, we can see that the Snellius' law contains n', "with n' representing the refractive index which, in the case of refraction into an absorbing medium, is a complex number $n' = n\,(1 - i\kappa)$; n stands for the real part of the refractive index, κ is a number called absorption index, as it is closely related to the phenomenon of absorption".

"Total reflection is accompanied by a wave motion with wave fronts perpendicular to the interface in both media. If the second medium is non-absorbing, the time average of the energy transfer from one medium to the other vanishes, and all incident energy is reflected. Microscopically, however, at any moment, one finds a periodic alternation of places where energy is transferred from the first to the second medium, with places where the energy stream flows in the opposite direction. If for the second medium $\kappa \neq 0$, it is therefore to be expected that the reflection will no longer be total, but that part of the incident radiation will be absorbed by the surface layers" (Fahrenfort, 1961).

The discussion that followed the presentation at the Meeting, 1959, is also interesting for applications. J. Zarzycki asked: "In the case of substances such as rubber etc. mentioned in your [Fahrenfort's] paper, how is the optical contact secured between the semicylindrical lens and the sample? Is it simply the pressure?" Fahrenfort: "In the case of elastically or plastically deformable samples the optical contact is most easily achieved by a slight pressure. In the case of harder materials, the introduction of a capillary layer of a highly refraction liquid such a CS_2 will ensure the contact. In some cases, the contact remains even after the evaporation of the liquid". Let us stress that the carbon disulfide is dangerous. The texts of the works proposed at the "Advances in molecular spectroscopy: proceedings by International Meeting on Molecular Spectroscopy. (4^{th}: 1959: Bologna and Rome)", 1962, published by Macmillan, New York, are available at the web archive https://archive.org/details/advancesinmolecu0002inte/page/n3/mode/2up

"The use of multi-reflectance attenuated total reflectance, in which the beam is internally reflected many times, was suggested by [Nicolas James] Harrick. Since attenuation occurs at each internal reflection the resulting spectrum will show a considerable amplification of weak absorptions when compared with a single reflection attenuated total reflectance spectrum. Various designs of analyzing crystals for obtaining multi-reflectance

attenuated total reflectance spectra have been suggested" (Baxter & Puttnam, 1965, mentioning Harrick, 1960, Hansen & Horton, 1964, and Harrick, 1964). In the article by Harrick, 1960, we find that "It has been suggested [note 1] that the physics and chemistry of surfaces of optically transparent materials, particularly semiconductors, may be studied through the analysis of the spectrum of totally internally reflected radiation"; in the note 1 of Harrick's article it is told: "Discussion by N. J. Harrick following paper by R. P. Eischens at Second Conference on Semiconductor Surfaces, Naval Ordnance Laboratories, White Oak, Maryland, December, 1959 [J. Phys. Chem. Solids (to be published).] It was brought to the author [Harrick]'s attention after the work described here was completed that Dr. J. Fahrenfort of the Royal Dutch Shell Laboratories, Amsterdam, has described what appears to be a similar technique to observe the spectra of organic materials on silver chloride at the Fourth International Congress on Molecular Spectroscopy, Bologna, September, 1959 (unpublished)". Then, we can add what told by Graf and coworkers, 1987, that the "Internal reflectance or attenuated total reflectance (ATR) spectroscopy [, which] is probably the second most commonly used infrared spectroscopy technique after transmission [, was originally] independently developed by Fahrenfort and Harrick". "One of the first applications was for the study of the surface and bulk properties of semiconductors" (Graf et al., 1987).

It was more than sixty years ago, that Jacob Fahrenfort - and Nicolas James Harrick too - "introduced attenuated total reflection (ATR) to investigate the infrared response of organic compounds. He [Fahrenfort] noticed that for absorbing materials characterized by a complex refractive index ... the internal reflection spectrum R resembles that obtained in the transmission mode in spectral regions, … Since ATR measurements are very sensitive and particularly advantageous for thick samples for which transmittance measurements are not possible, log R^{-1} was commonly used as a representation for an absorption spectrum" (Mendoza-Galván et al., 2021).

The discussion about the ATR principle continues in Appendix B.

Discussion

Mentioning the presence of the evanescent field in the total internal reflection phenomenon, Subramanian and Rodriguez-Saona, 2009, summarize the ATR method telling that "Some amount of the light energy escapes the crystal and extends a small distance (0.1–5 μm) beyond the surface in the form of waves". Because of energy absorption, "the intensity of the reflected light reduces" producing an *attenuated total reflectance* (Subramanian & Rodriguez-Saona, 2009). Moreover, the "evanescent field depends strongly on the angle of incidence of the incident beam. … [it] also varies as a function of frequency of the radiation. ... The greater the frequency, the faster the decay of the field. As a result, the evanescent field, at a greater frequency, decays to zero at a shallower depth than that at a lower frequency" (Ekgasit & Padermshoke, 2001).

In QD-Europe, it is stressed that an ATR spectrum is "different to that obtained for the same sample when collected as a transmission spectrum", since measurement methods are different, being differences dictated "by the fundamental way the sample information is being collected". In transmission spectroscopy, the light passes through the sample, "whereas ATR spectroscopy is the interaction of light by passage into the surface of a sample species. *Note that neither method can be regarded as giving the "correct" spectrum – they are simply different*" (QD-Europe). The web site details the role of wavelength and refractive index on the penetration depth of the light. Also, the differences of intensities, the band shift, and the band asymmetries that we observe when an ATR spectrum is compared to a transmission spectrum, are discussed. For instance, regarding the band distortion, it is told that "sometimes in ATR measurements the absorption bands can become *slightly asymmetric* compared to the bands seen in transmission measurements" (QD-Europe). The deformation of the band shape is due to "the rapid change of refractive index of the sample across the band". "The refractive index of the sample varies from a low value on the short wavelength side of the band to a high value on the long wavelength side. This causes the effective penetration depth to also rapidly increase toward the long wavelength side and causes the characteristic shape of the bands seen" (QD-Europe).

Let us consider also the observations made by Elsebeth Kendix, 2009: “in most cases comparison of standard spectra collected in FIR transmission and FIR ATR mode leads to only a few differences. The most obvious, when comparing transmission with ATR, is the distortion of band shape. The ATR band shape appears *asymmetrical* in the lower wavenumber region when compared to spectra collected in transmission mode. Also, *intensity differences* are noticed. However, the biggest difference can be the *shift* of strong absorbing bands moving to lower wavenumbers in ATR mode” (Kendix, 2009). Usually, “the shifts observed are small, approximately 1-10 cm^{-1}, but for very strong absorbing compounds the shifts observed can be as big as 30-50 cm^{-1}” (Kendix, 2009). Then the ATR spectra can be “considerably different from transmission spectra with respect to intensities, band shift and band distortions” (Kendix, 2009). If we could use both techniques, we could obtain databases, for instance, to “identifying unknown pigment samples” (Kendix considers pigments in the framework of analyses of cultural heritage materials). “Perhaps it would be less time consuming and more convenient to try to correct the ATR spectrum to simulate a transmission spectrum by using a correction algorithm” (Kendix, 2009). Besides advanced ATR correction algorithms, we could “try applying the Kramers-Kronig transformation on the ATR spectra”. However, “the transformation of spectra are usually problematic”. Kendix proposes an example of transformations with algorithm and KK relations on cinnabar ATR spectrum, concluding that it is better to collect both transmission and ATR spectra “to build a database for comparison with unknown samples using both techniques as means of detection and identification”.

As given in literature, the ATR measurement method is producing intrinsically asymmetric bands, and therefore, for the deconvolution of the spectrum, an asymmetric band shape is required. We will show that, using the asymmetric q-BWF functions, we can determine the components of ATR spectra, useful for comparison with infrared data available from literature.

Air gap

“A drop of water on the ATR crystal before contact with the solid sample can enhance the signal intensity when there are problems achieving contact due to planarity issues. But the question is if the sample can tolerate the exposure to water” (Kendix, 2009). In fact, as stressed by Ekgasit and Padermshoke, 2001, “the evanescent field is greatly altered by the air gap. … Absorbance of the system with an air gap is always smaller than that with the optical contact since the region near the internal reflection element surface, where the field is strongest, is occupied by an air gap that does not involve any absorption. The sample, which is positioned at a distance far from the internal reflection element, experiences a much smaller evanescent field compared to a system with optical contact. The absorption decreases as the air gap is widened”. Therefore, the “optical contact between an internal reflection element (IRE) and a sample is crucial for obtaining a good spectrum in an attenuated total reflection (ATR) experiment. … Two techniques for determining the goodness of contact are proposed [by Ekgasit and Padermshoke] - first, by making a comparison between polarized ATR spectra and, second, by making a comparison between ATR and transmission spectra” (Ekgasit and Padermshoke, 2001).

The ATR-spectroscopy, “at the end of the 5th decade and the beginning of the 6th decade of the previous century”, started being widespread used “for structural investigation especially of liquids and soft solids like polymers, etc. For samples with hard surfaces, e.g. most of the inorganic single crystals, ATR-spectroscopy leads a *shadowy existence* due to the need of establishing an intimate contact between the incidence medium (i.e. the ATR-crystal) and the medium under investigation (the sample)”, as noted by Ivanovski and coworkers, 2009. “Devlin et al. solved this problem by growing their samples directly onto the ATR-crystal, a technique, which is, however, applicable only in rare cases. Piro et al. used, in addition to the application of high pressure, KRS-5 as ATR-crystal, which is a comparably soft material, but criticized the occurrence of light scattering losses as result of surface damages or scratches due to the softness. Deane et al. also employed a KRS-5 ATR-crystal but additionally utilized methylene iodide saturated with sulphur as an immersion fluid to reduce the scattering losses” (Ivanovski et al., 2009). Having this fluid a problem of toxicity, “a quite remarkable technique to establish intimate contact is the use of so-called thermoplastic glasses as denser medium, e.g. low melting chalcogenide glasses” (Ivanovski et al., mentioning Zolotarev, 2000). Ivanovski and coworkers aim “to introduce a technique that is easy to apply and assure optical contact using a non-toxic, non-volatile and

easily removable coupling agent". They propose the use of a "thin polyethylene layer used as contacting agent". The layer is produced using commercial PE, "firstly dissolved in boiling CCl_4. .... Precautions in handling the toxic and volatile CCl_4 were taken into account. After the preparation of the solution, it was cooled and then applied on the sample surface, which was in the next step pressed against the ATR crystal" (Ivanovski et al., 2009). In the case of transparent sample, the "visual evidence of the established optical contact was the appearance of the single crystal shape on the bottom of the ATR semi-sphere" (Ivanovski et al., 2009).

In Paschotta, for the RP Photonics Encyclopedia, we can find told that "when two transparent solid pieces with highly flat and clean surfaces are put into close contact, they will form a solid connection (bond), where they are firmly held together by intermolecular forces such as Van der Waals forces and hydrogen bonds. It may not be necessary to apply a high pressure, as the pieces naturally join. … there are methods of optical contact bonding, which essentially involve particularly careful polishing and cleaning of the surfaces, reaching a surface flatness on nanometer dimensions. Optical contact bonding methods do not involve the use of a contact agent such as an optical glue; they are adhesive-free. … Simply pressing the parts together with moderate pressure may be enough, but higher pressure is applied in some cases" (Paschotta, 2024). Some methods are illustrated by Paschotta, who is concluding that "generally, this kind of bonding is more labor-intensive and costly than adhesive-based techniques due to the extreme precision requirements". In the case of spectroscopy, the glue is adding their absorption bands.

In the case of RRUFF ATR powder samples, the contact is obtained by pressure. Let us pass to propose some examples of RRUFF spectra (Raman and ATR).

Azurite and malachite

Grinded azurite and malachite minerals were widely used in the past to create pigments. "Azurite was known in the pre-classical ancient world". It was used in ancient Egypt and Greece, "for example on the Acropolis in Athens" (Wikipedia, mentioning R. J. Forbes, 1955). "Pliny and Vitruvius describe the more common compounds" used for pigments, with names that today we can translate "as azurite, lazurite, chrysocolla, indigo and Egyptian blue for blues and verdigris, malachite, celadonite, glauconite and chlorite for greens" (Jorge-Villar & Edwards, 2021). Jorge-Villar and Edwards used Raman spectroscopy to identify blue and green Roman pigments. Bicchieri and coworkers, 2001, used micro-Raman to study azurite and lapis-lazuli in the pigments of illuminated medieval manuscripts. Han and coworkers, 2016, investigated the Raman spectra of azurite pigments of several particle-size groups. "The linewidths of the phonon modes ∼400 cm^{-1} of azurite powders were found to increase as the particle sizes get smaller" (Han et al., 2016).

Regarding minerals, azurite and malachite Raman and infrared spectra had been studied by Frost et al., 2002. "Azurite [$Cu^{2+}{}_3(CO_3)_2(_{OH})_2$] and malachite [$Cu^{2+}{}_2(CO_3)(OH)_2$] are both monoclinic hydroxy carbonates of copper" (Frost et al., 2002). "The spectra of both azurite and malachite contain modes of three separate vibrational groups: OH, CO_3 and Cu–O". The OH-stretching modes are between 3400 and 3475 cm^{-1}. The OH bending modes are between 875 and 1045 cm^{-1}. The carbonate group displays bands observed "at 1090 cm^{-1} (v_1), 837 and 817 cm^{-1} (v_2), 1490 and 1415 cm^{-1} (v_3) and 769 and 747 cm^{-1} (v_4). … IR bands for the Cu–O stretching modes are observed at 495 and 400 cm^{-1}, while Cu–O bending modes occur at 455 and 345 cm^{-1}. Bands at 305 and 240 cm^{-1} are assigned to the O–Cu–OH bending modes. The Raman out-of-plane bending modes are found at 194 and 170 cm^{-1}. For the carbonate group, infrared bands are observed at 1095 cm^{-1} (v1), 834 and 816 cm^{-1} (v_2), 1430 and 1419 cm^{-1} (v_3) and 764 and 739 cm^{-1} (v_4)" (Frost et al., 2002).

Regarding the hydroxyl-stretching bands, "the Raman spectrum of azurite displays an intense sharp band at 3453 cm^{-1}. This band is complex and may be resolved into an additional low intensity component at 3427 cm^{-1}". "The Raman spectrum of malachite shows a broader band in this region with bands observed at 3468 and 3386 cm^{-1} at 298 K". The infrared spectra "confirm the complex nature of the hydroxyl-stretching region of these two minerals. … The combination of the data from the Raman and infrared spectroscopic analyses proves the *non-equivalence* of the hydroxyl units in the azurite and malachite structure" (Frost et al., 2002). Let us start from azurite, with the deconvolution of Raman RRUFF R050497 broad scan.

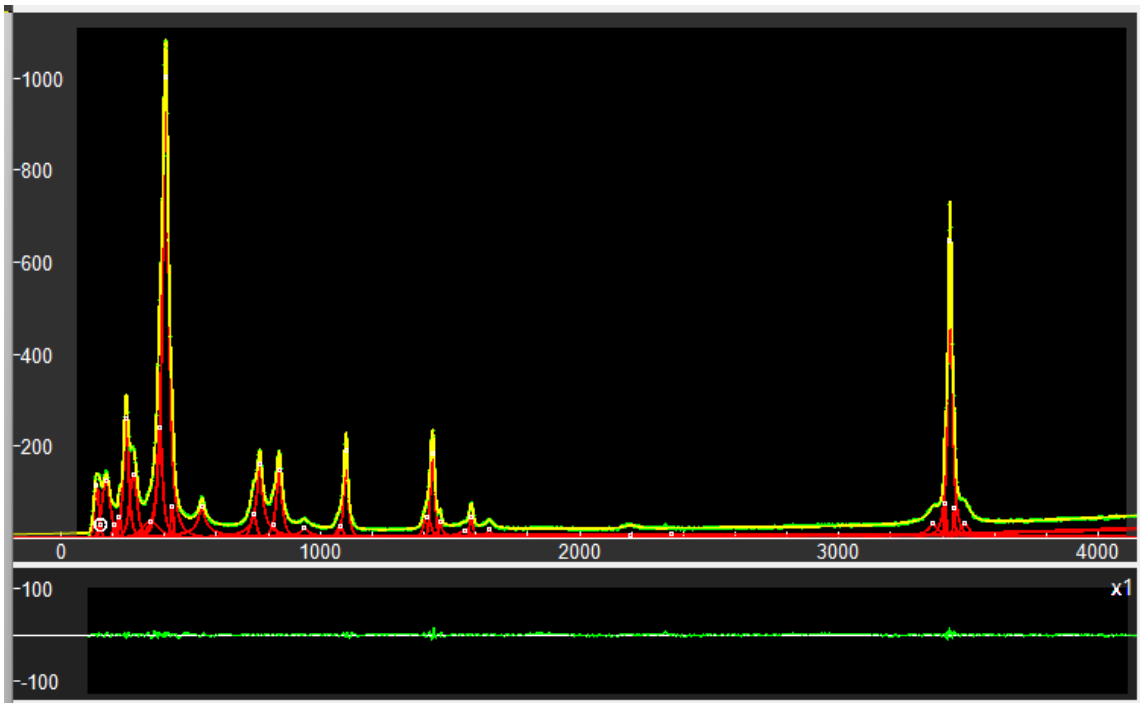

Fig.1a: Deconvolution of azurite RRUFF R050497 Raman broad scan spectrum. It is decomposed into q-Gaussian bands (red curves). For the q-Gaussian functions, see please the Appendix. The lower part of the image is showing the misfit, that is the difference between data (green) and the sum of components (yellow curve). On x-axis, we have the wavenumbers in cm^{-1}. Note the large hydroxyl-stretching band.

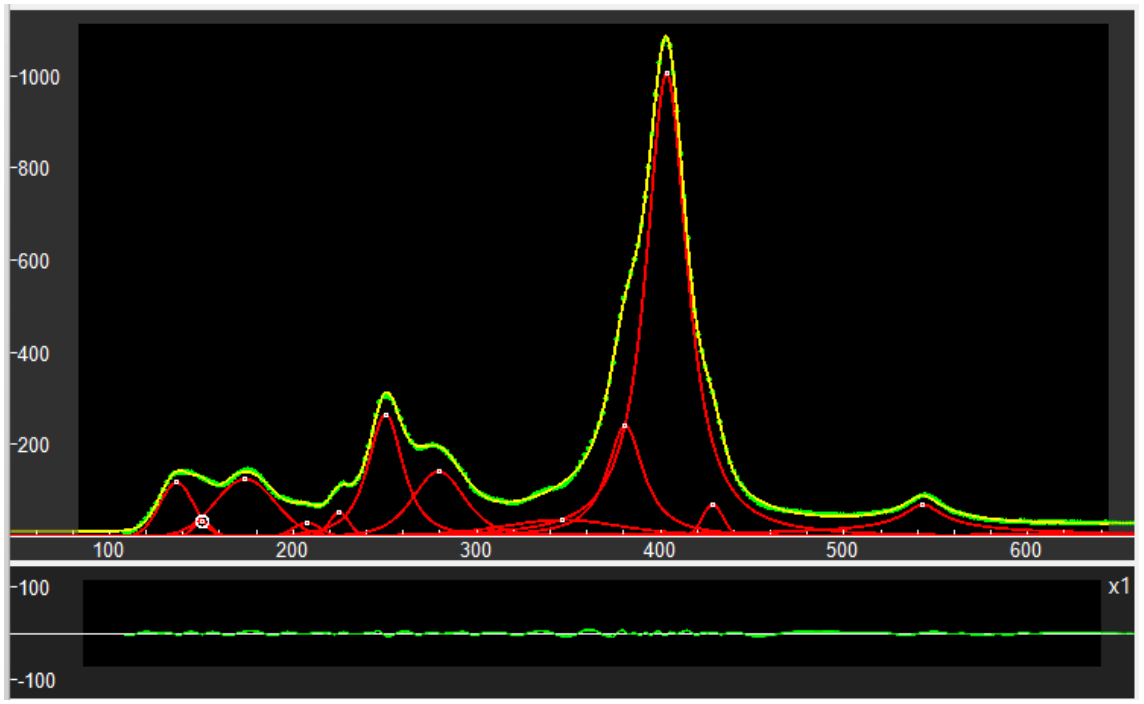

Fig.1b: Detail of the deconvolution of azurite RRUFF R050497 broad scan spectrum.

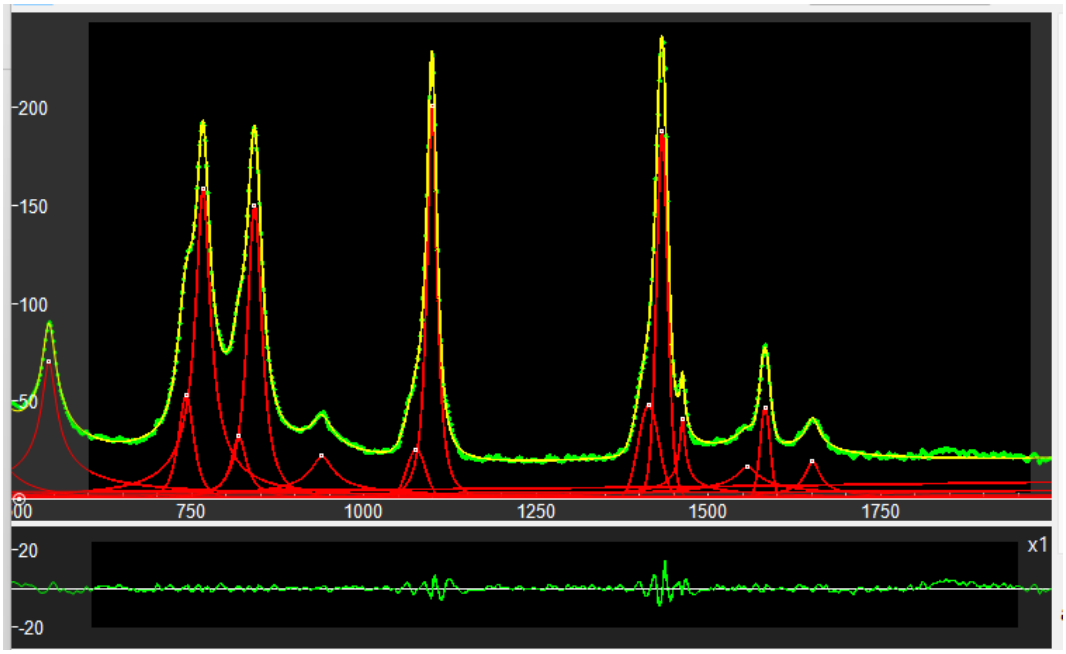

Fig.1c: Another detail of the deconvolution of azurite RRUFF R050497 broad scan spectrum.

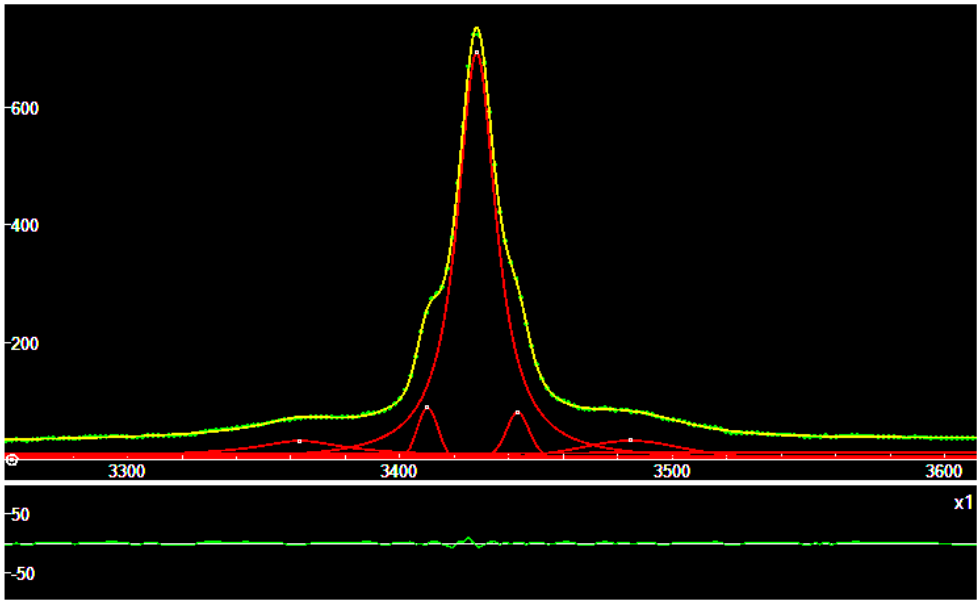

Fig.1d: OH-stretching region of azurite RRUFF R050497 broad scan spectrum.

The plots in the Figs.1a-d, and the figures that will follow in the text, have been obtained by means of software Fityk (Wojdyr, 2010), after defining in it the q-Gaussian functions (see Appendix A for further details). By means of the data obtained from q-Gaussian deconvolution, we can compare the Raman shift (cm^{-1}) of the centers of components given in the Figure 1, with the results given in literature.

Table I: Raman shift (cm^{-1}) of the centers of the components as in our Figs.1a-d. Bold numbers represent the relevant components that we can easily see in the Fig.1a, "sh" means "shoulder".

136 150 175 207 226 ***250*** ***279*** *341* ***381*** *(sh)* ***403.5****(strongest) 428* ***543*** *742* ***766.5*** *818.5* ***841*** *939 1075.5* ***1098.5*** *1413* ***1433*** *1462* ***1582*** *1651 3363 3410* ***3428*** *(strong) 3443 3484.5*

Let us consider the ATR-IR spectrum and the deconvolution with q-BWF functions.

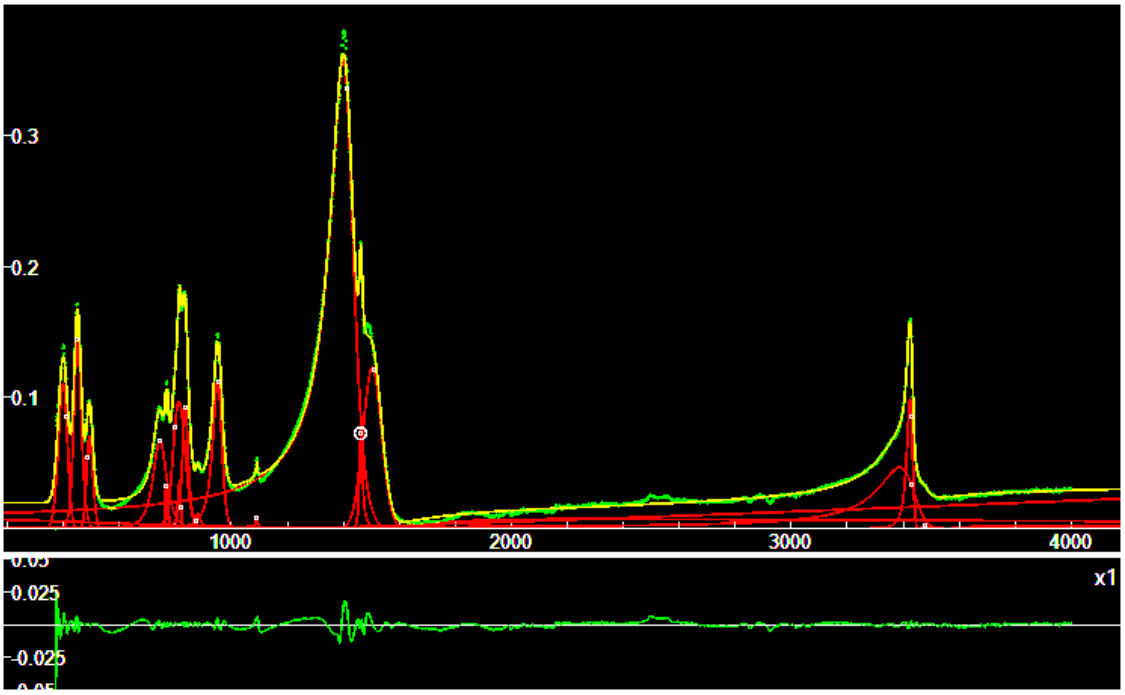

Fig.2a: Deconvolution of azurite RRUFF R050497 ATR-IR spectrum. It is decomposed into q-BWF band shapes (red curves). For the q-BWF functions, see please the Appendix A. The lower part of the image shows the misfit, that is the difference between data (green) and the sum of components (yellow curve). On x-axis, we have the wavenumbers in cm^{-1}.

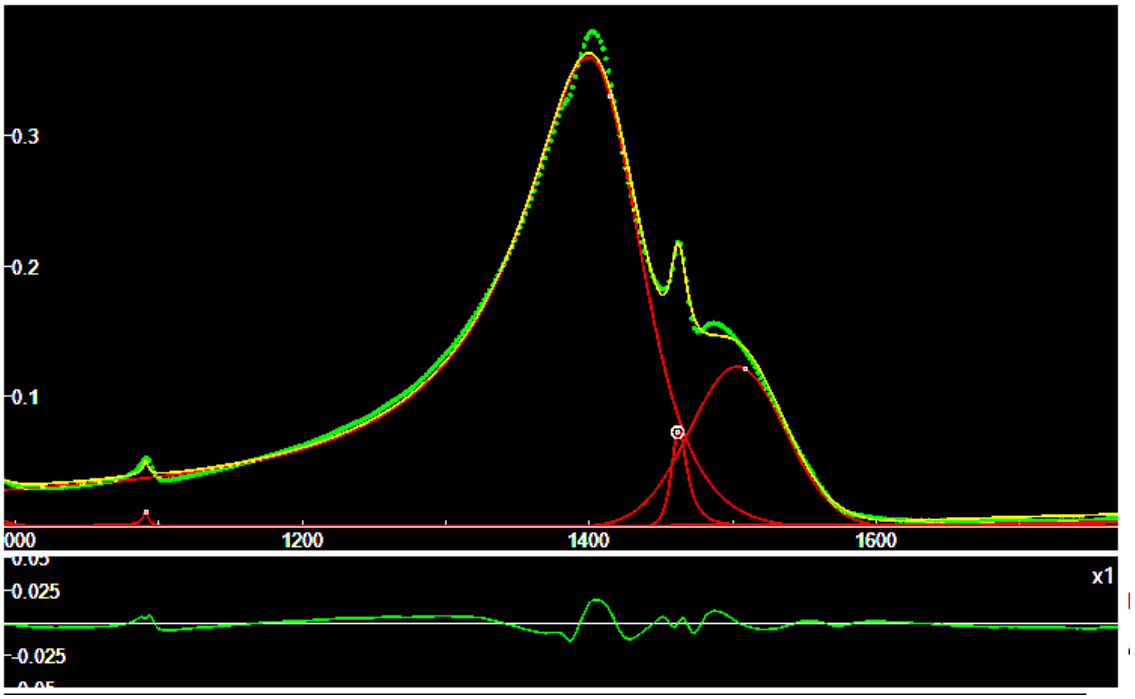

Fig. 2b: A detail of the main peak in Fig.2a.

Note that the position of the center of a q-BWF function is different from the position of its peak. Here in the following Table II we propose the positions of the q-BWF peaks.

Table II: ATR-IR shift (cm^{-1}) of the peaks of the components as in our Figs.2a-b.

398 ***450*** ***493*** ***745*** ***769*** *812* ***814*** ***835*** *880* ***950*** ***1091*** *1400* ***1462*** *1504* *3388* ***3425***

At the web-page https://spectra.chem.ut.ee/paint/pigments/azurite/, database of the Institute of Chemistry University of Tartu, Estonia (Vahur et al., 2016), we can find the following peaks.

Table III: ATR-IR shift (cm^{-1}) of peaks as in the database of the University of Tartu. The bold numbers are very close to the bold values in Table II.

250 301 342 ***401*** ***447*** ***491*** *694* ***743*** ***769*** ***815*** ***833*** ***950*** *1010 1029* ***1092*** *1412* ***1463*** *1494*

3425 *3619 3694*

Let us pass to the malachite sample.

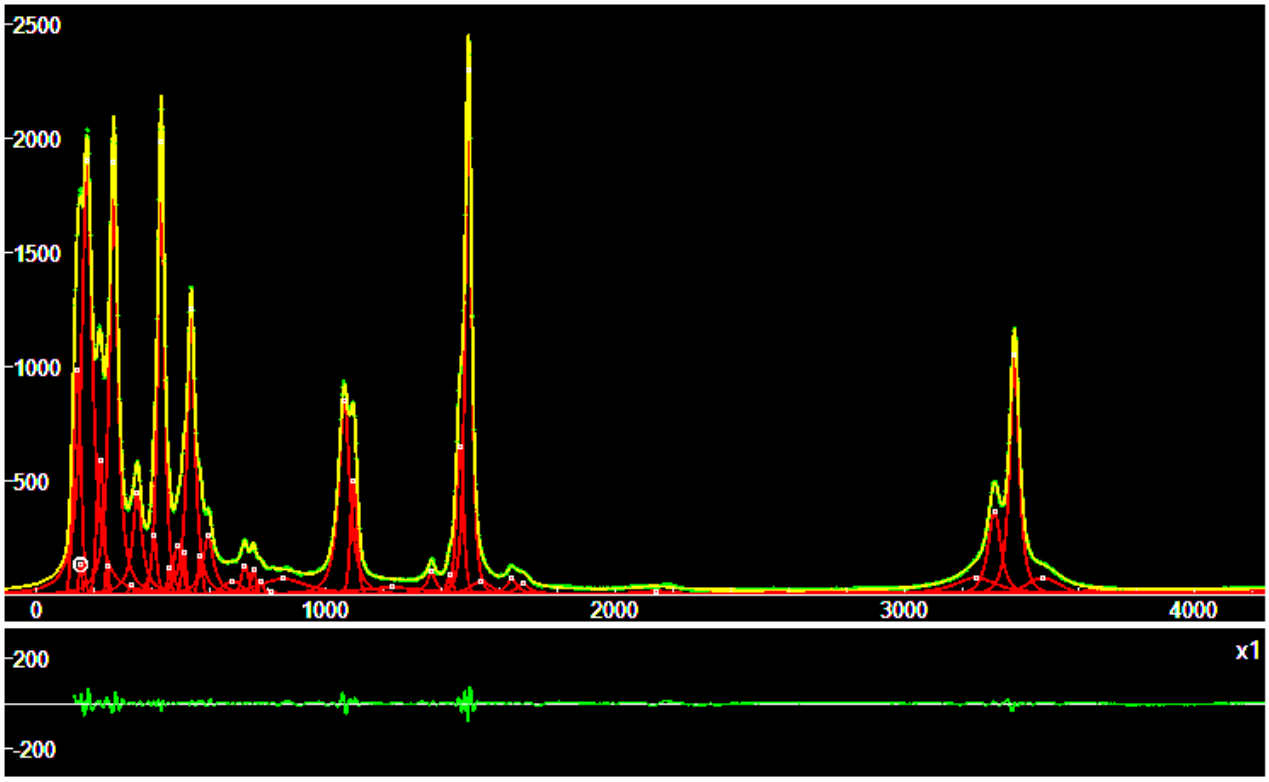

Fig.3a: Deconvolution of malachite RRUFF R050508 Raman broad scan spectrum, decomposed into q-Gaussian bands (red curves). The lower part of the image shows the misfit, that is the difference between data (green) and the sum of components (yellow curve). On x-axis, we have the wavenumbers in cm^{-1}.

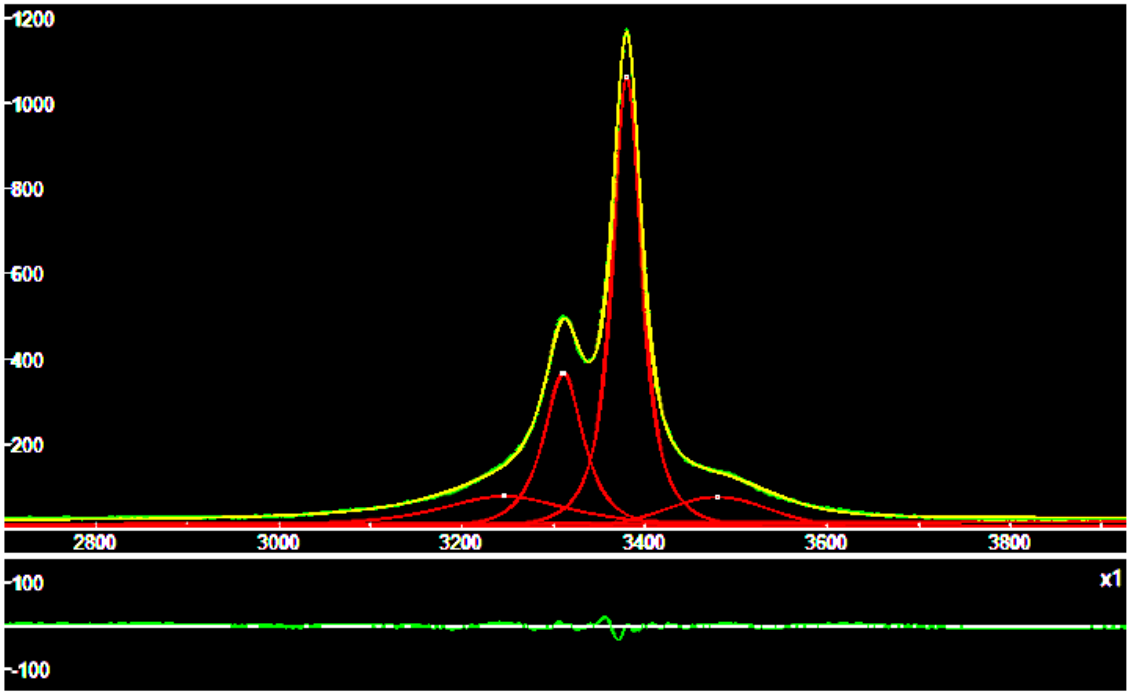

Fig.3b: OH-stretching region of malachite RRUFF R050508 broad scan spectrum.

Table IV: Raman shift (cm^{-1}) of the centers of the components as in our Figs.3a-b. Bold numbers represent the relevant components that we can easily see in the Fig.3a, "sh" means "shoulder".

141.5 ***175.5*** *(strong)* *221* *245* ***276.5*** *(strong)* *349.5* *407 (sh)* ***432*** *(strong)* *461 (sh)* *490* *510 (sh)* ***535*** *566.5 (sh)* *594.5* *678.5* *721* *751* *775* *852* ***1064*** ***1097.5*** *1366* *1429* *1464 (sh)* ***1494*** *(strongest)* *1537* *1643.5* *1682* *3246.5* ***3311*** ***3380.5*** *(strong)* *3480*

We can compare the components of the OH-stretching Raman region of azurite and malachite, as in the following Table V.

Table V: Raman shift (cm^{-1}) of the centers of the components of the OH-stretching region.

Azurite			*3363*	*3410*	*3428*	*3443*	*3484.5*
Malachite	*3246.5*	*3311*	*3380.5*				*3480*

Let us pass to the ATR spectrum of malachite.

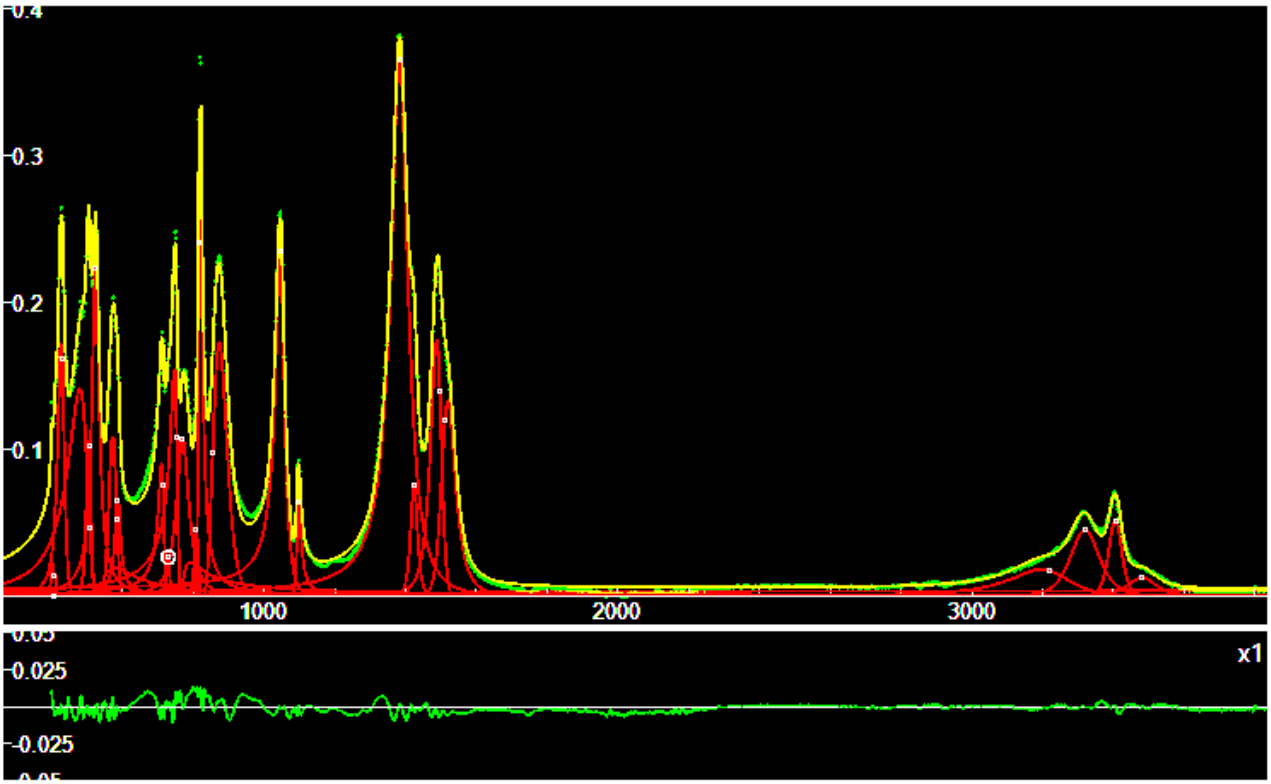

Fig.4: Deconvolution of malachite RRUFF R050508 ATR-IR spectrum into q-BWF band shapes.

TableVI: ATR-IR shift (cm^{-1}) of the peaks of the components as in our Fig.4.

426 480 506 ***523.5*** ***572*** *586* ***711*** *727 747 769 807.5* ***819*** *873* ***1045*** ***1097*** ***1383*** *1423* ***1487*** *1520 3196 3319 3406.5 3481*

At the web-page https://spectra.chem.ut.ee/paint/pigments/malachite/ , database of the Institute of Chemistry University of Tartu, Estonia (Vahur et al., 2016), we can find the following peaks.

Table VII: ATR-IR shift (cm^{-1}) of peaks as in the database of the University of Tartu. The bold numbers are very close to the values in Table VI.

258 354 426 501 ***523*** ***570*** ***711*** ***747*** *775* ***817*** *868* ***1043*** ***1096*** ***1384*** ***1489*** *3310 3393*

Siderite and rhodochrosite

"Siderite ($FeCO_3$) and rhodochrosite ($MnCO_3$) are two interesting carbonate minerals, which normally occur in hydrothermal deposits on deep-sea altered oceanic crust" (Wang et al., 2023). In Makreski and Jovanovski, 2003, we can find a study of some orthorhombic carbonates by FTIR spectroscopy. Regarding siderite, we can find bands as (cm^{-1}): 1421 (v_3), 866 (v_2) and 731 (v_4). In Zhu et al., 2021, we find data about infrared spectral characteristic of carbonate minerals (MCO_3, M= Mg, Ca, Mn, Fe). In their Table 3, we find (cm^{-1}): Siderite, 733 (v_4), 866 (v_2), 1426 (v_3), 1811, 2496, 2852, Rhodochrosite 725 (v_4), 864 (v_2), 1422 (v_3), 1799, 2492, 2849.

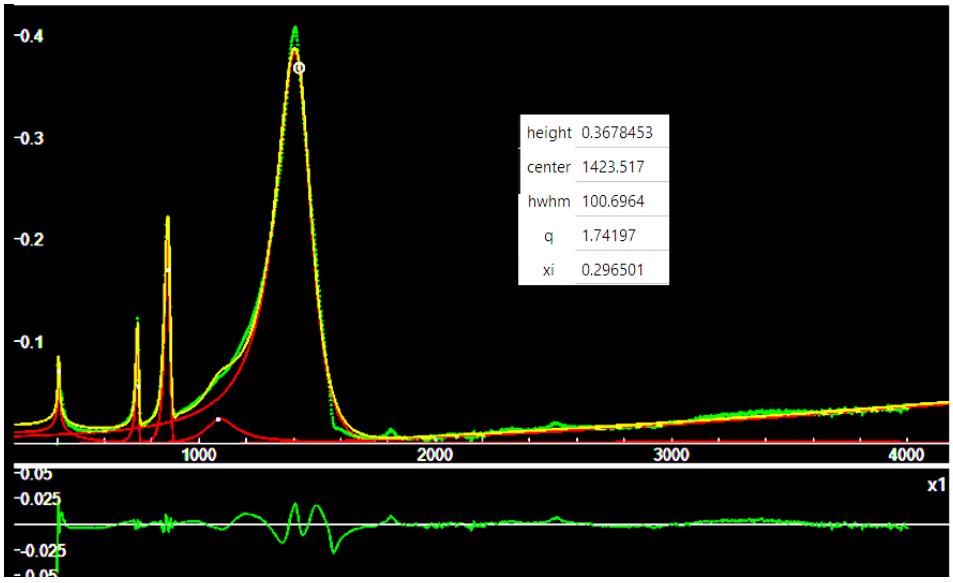

Fig. 5: Deconvolution of siderite RRUFF R040034 ATR spectrum, decomposed into q-BWF functions. Insert in the figure is giving parameters of the q-BWF function. Let us stress that the center of the q-BWF function (the white marker) does not correspond to the position of the peak.

In Figure 5, we deconvoluted the siderite RRUFF R040034 ATR spectrum in q-BWF functions. These functions are fundamental to describe the trend of the spectrum; if we use for the deconvolution the split-q-Gaussians for instance (see Appendix A), such as other split functions, it is impossible to obtain the trend of the spectrum. From the insert in the Figure 5, we can find that the q-parameter of the q-BWF function of the main band is equal to 1.74; let us remember that for q equal to 2, we have a BWF function, that is an asymmetric form, according to Fano, of a Lorentzian function. When q is close to 1, we have an asymmetric Gaussian function. In the case shown in Figure 5, we are closer to an asymmetric Lorentzian function.

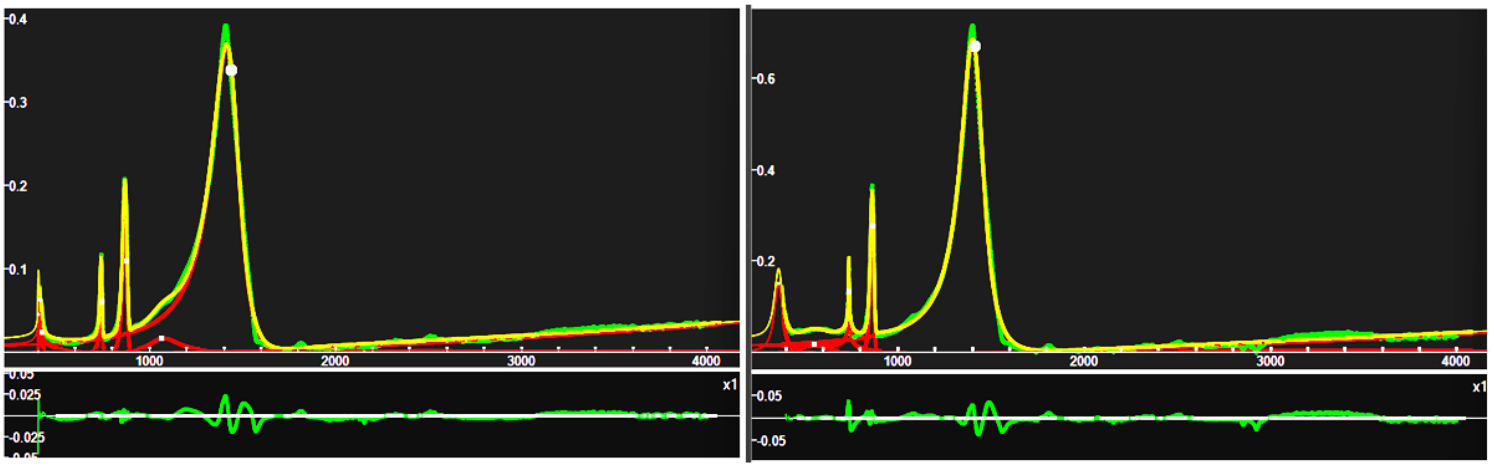

Fig. 6: Deconvolution of siderite RRUFF R050262 *ATR spectrum, decomposed into q-BWF functions (left panel). The q-parameter of the q-BWF main peak (left) is equal to 1.70. Deconvolution of siderite RRUFF* R050349 *ATR spectrum, decomposed into q-BWF functions (right panel). The q-parameter of the q-BWF main peak (left) is equal to 1.86.*

Further siderite examples are proposed in Figure 6. The following figure is regarding rhodochrosite.

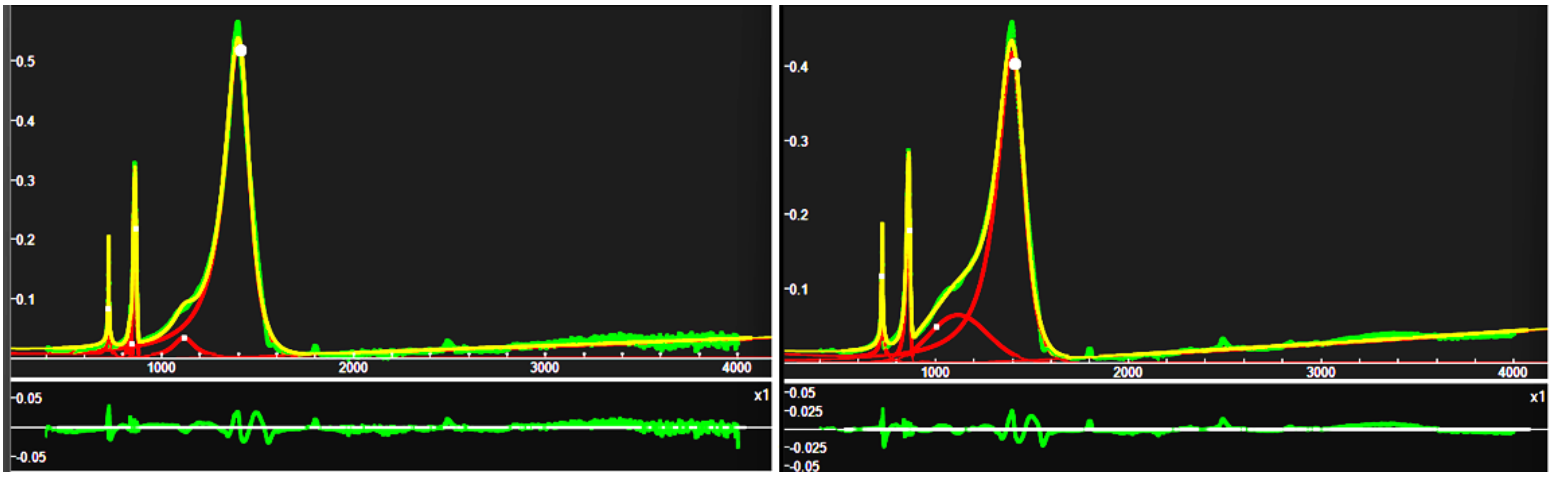

Fig. 7: Deconvolution of rhodochrosite RRUFF R040133 *ATR spectrum, decomposed into q-BWF functions (left panel). The q-parameter of the q-BWF main peak (left) is equal to 1.75. Rhodochrosite RRUFF* R050019 *ATR spectrum, decomposed into q-BWF functions (right panel). The q-parameter of the q-BWF main peak (left) is equal to 1.65.*

To improve the fit, we can add further components, such as in the two examples given below.

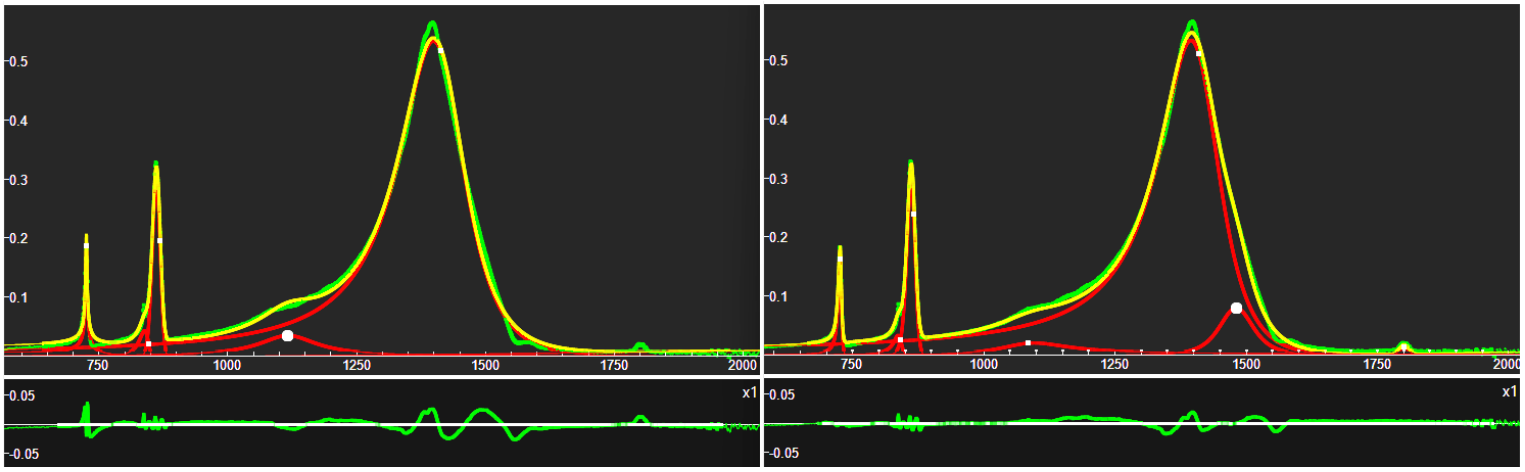

Fig. 8: Deconvolution of rhodochrosite RRUFF R040133 *ATR spectrum, decomposed into q-BWF functions as in Figure 7. In the right panel, a further q-BWF component is added on the right of the main peak.*

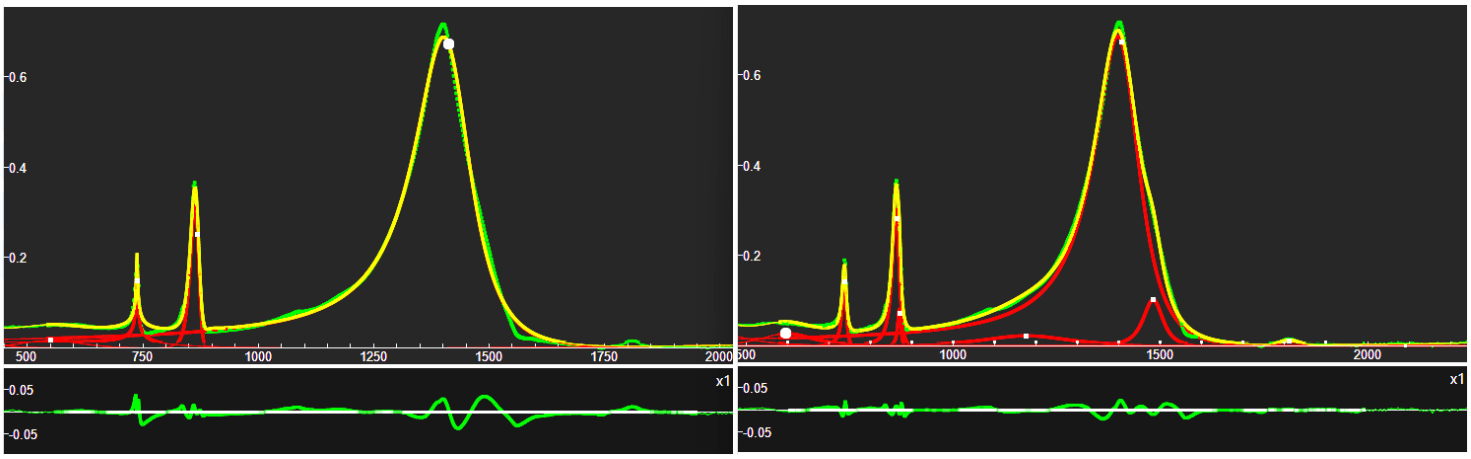

Fig. 9: Deconvolution of siderite RRUFF R050349 *ATR spectrum, decomposed into q-BWF functions (as in Figure 7). In the right panel, two further q-BWF components have been added to the main peak*

As shown in the examples proposed in Figures 8 and 9, we could add further components to improve the fit. However, a question exists: are these components true shoulders of the peak, produced, for instance, by defects in the material? In the following section, we propose some cases where true shoulders exist for sure.

RRUFF barite and carbonate minerals – We have already proposed the analyses of some RRUFF ATR spectra of barite-group and carbonate minerals. Here we show just some deconvolutions, from those given at the previous links. Some cases that we are here reporting have the main band, deconvolutes with two or more q-BWF components. Comparison with data in literature tells us that these components truly exist.

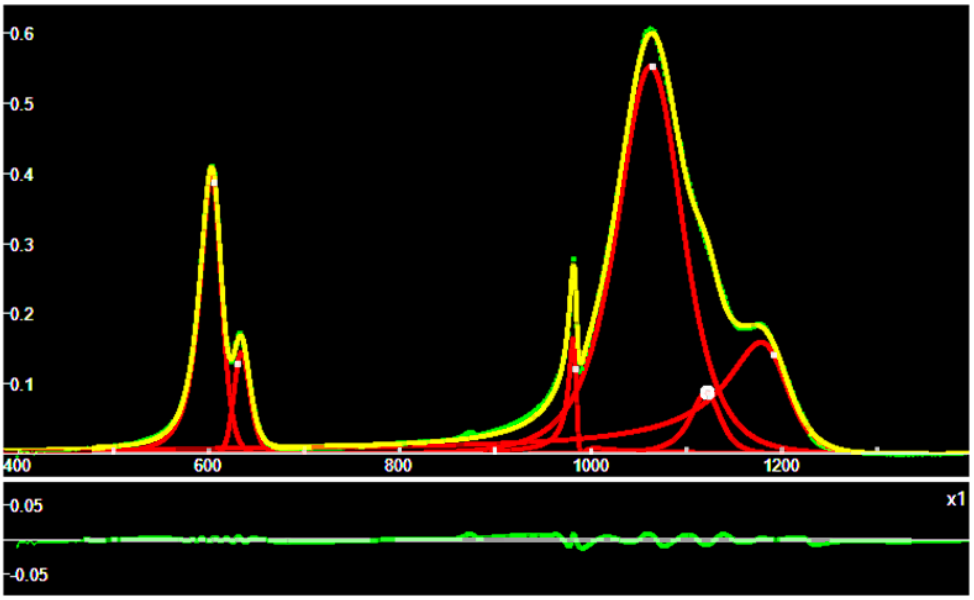

Fig.10: Deconvolution of baryte RRUFF R040036 ATR spectrum.

In the NIST Chemistry WebBook, we can find the barite infrared spectrum. We can use the transmittance /absorbance, to determine the peaks. The peaks are at (cm^{-1}): 615, 654, 987, 1077, 1128 and 1192. From the q-BWF deconvolutions that we have proposed in our previous discussion, we find (position of the peaks of the components, in cm^{-1}):

R040036	602	634		981	1062	1122	1180
R050335	602	634		981	1061	1120	1180
R050342	602	634		982	1063	1126	1181
R050375	602	634	967	981	1060	1119	1180
NIST	615	654		987	1077	1128	1192

Comparing the positions of q-BWF peaks with the NIST peaks, we can find a shift of the positions.

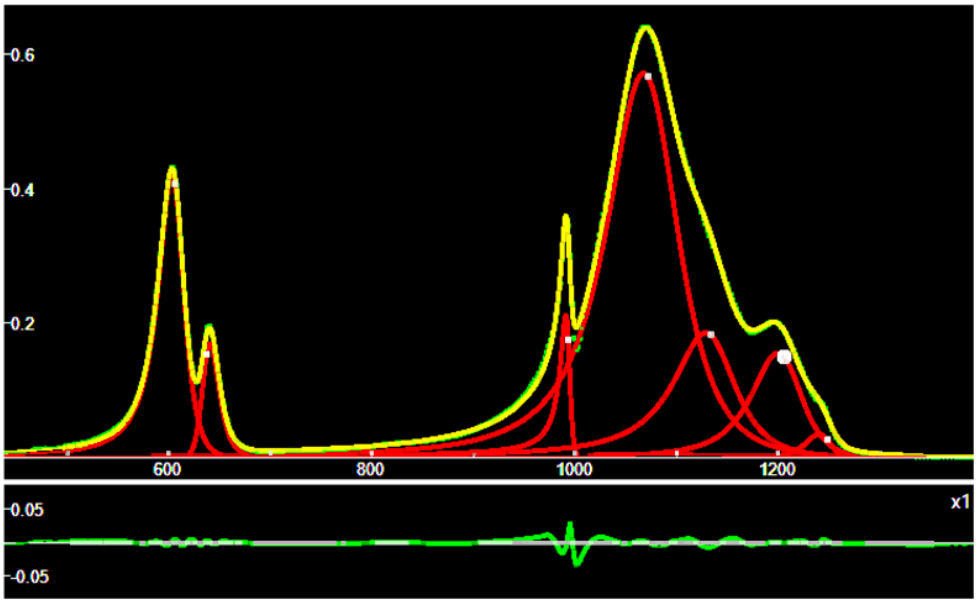

Fig.11: Deconvolution of celestine RRUFF R040007 ATR spectrum.

The same happens for celestine (an example is given in Figure 11). Again, as shown before, the web site spec4gem allows us to compare its data with our deconvolutions (in cm^{-1}):

R040007 (peaks)	603	640		991	1067	1130	1200	1240
R040007 (centers)	606	637		993	1072	1133	1206	1248
R050008 (peaks)	603	641		992	1063	1124	1200	1244
R050008 (centers)	605	638		995	1968	1128	1206	1246
SPEC4GEM	615	643	654	991	1098	1148	1198	1250

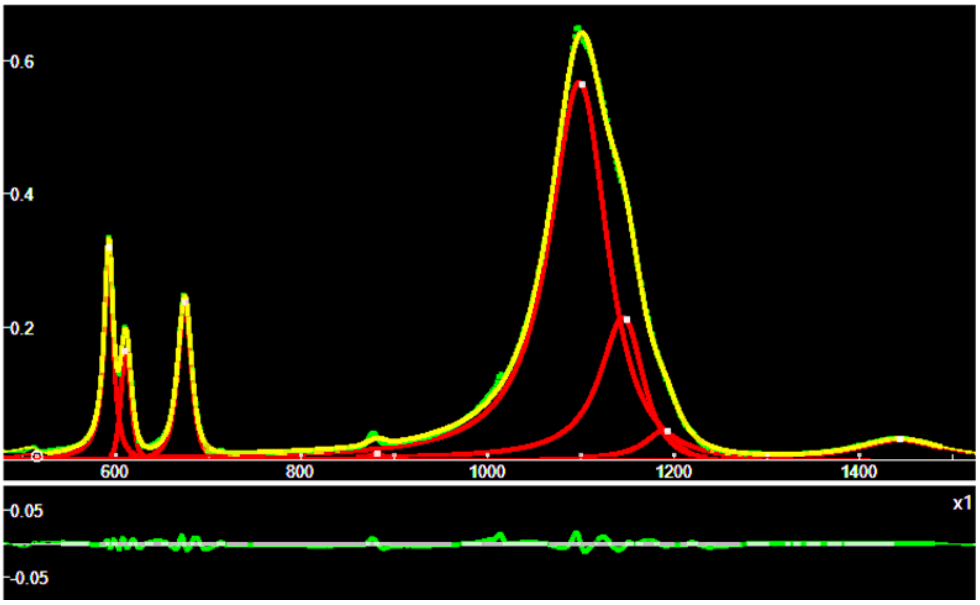

Fig.12: Deconvolution of anhydrite RRUFF R040012 ATR spectrum.

For anhydrite (as in Figure 12), and from the positions of the q-BWF peaks of the two spectra that we find in the RRUFF database, we can obtain (in cm^{-1}) a comparison with Prasad et al., 2005.

R040012	593	611	674	1100	1148	1191	1443
R040061	592	610	678	1093	1143	1193	
Prasad et al., 2005	595	615	676	1014	1124	1157	

Among the spectra of the carbonate materials, we can choose further examples. For instance, ankerite (Figure 13) has the main peak the fit of which can be improved adding a component, as in the cases of siderite and rhodochrosite. Aragonite (Figure 14) and bastnäsite-(Ce) (Figure 15) have a very good q-BWF main peak.

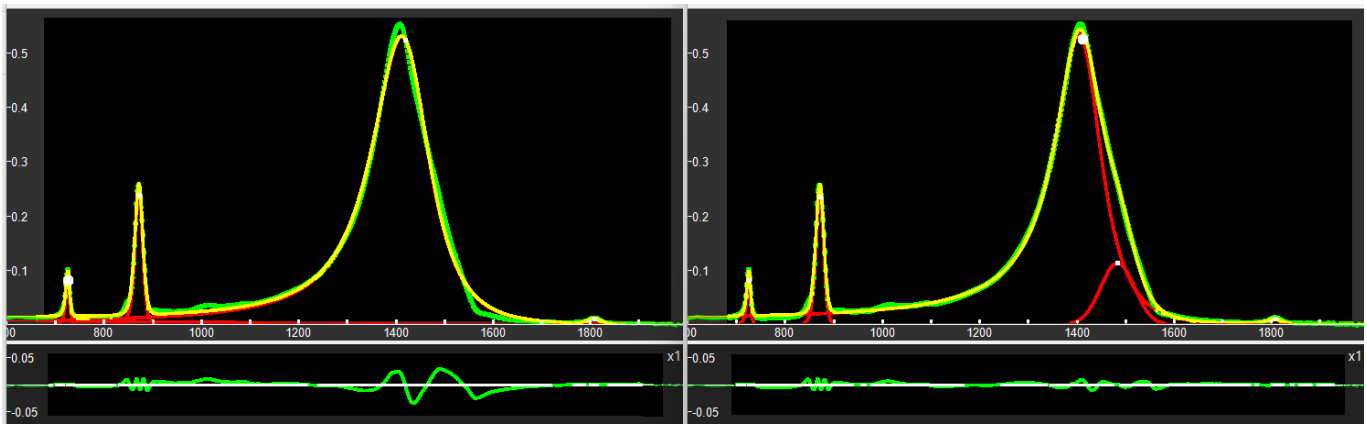

Fig.13: Deconvolution of ankerite RRUFF R050181 ATR spectrum. On the left, one q-BWF component is used for the largest peak. On the right, two q-BWF functions are used for this peak, to reduce the misfit. Consequently, we have the main component at 1404 cm^{-1}, and a "shoulder" at 1483 cm^{-1}.

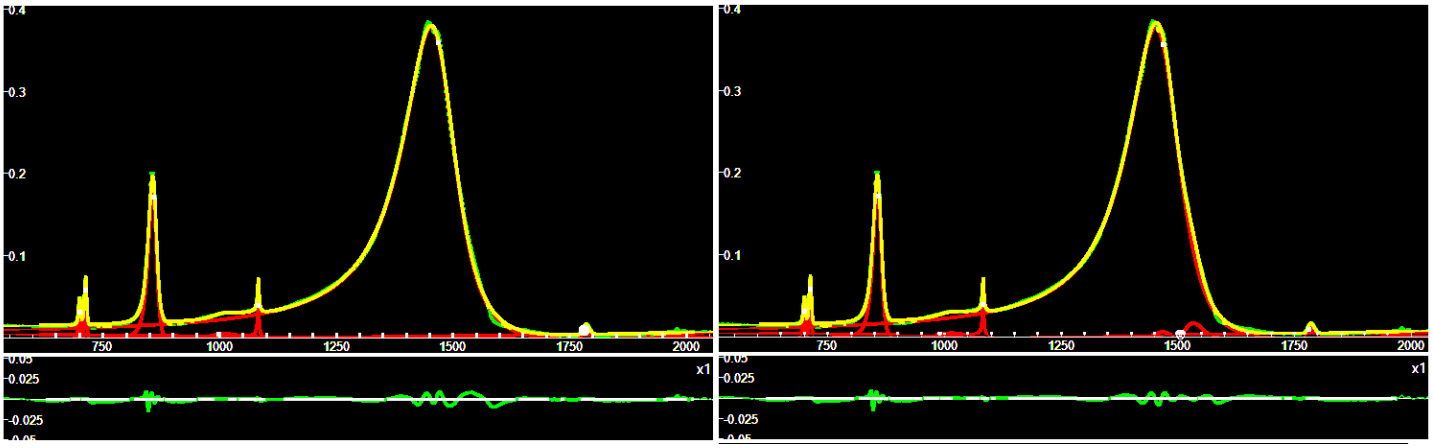

Fig.14: Deconvolution of aragonite RRUFF R040078 ATR spectrum. On the left, one component is used for the main peak. On the right, a second component is added. We can see that this further component has a very small effect. Therefore, we do not consider its presence.

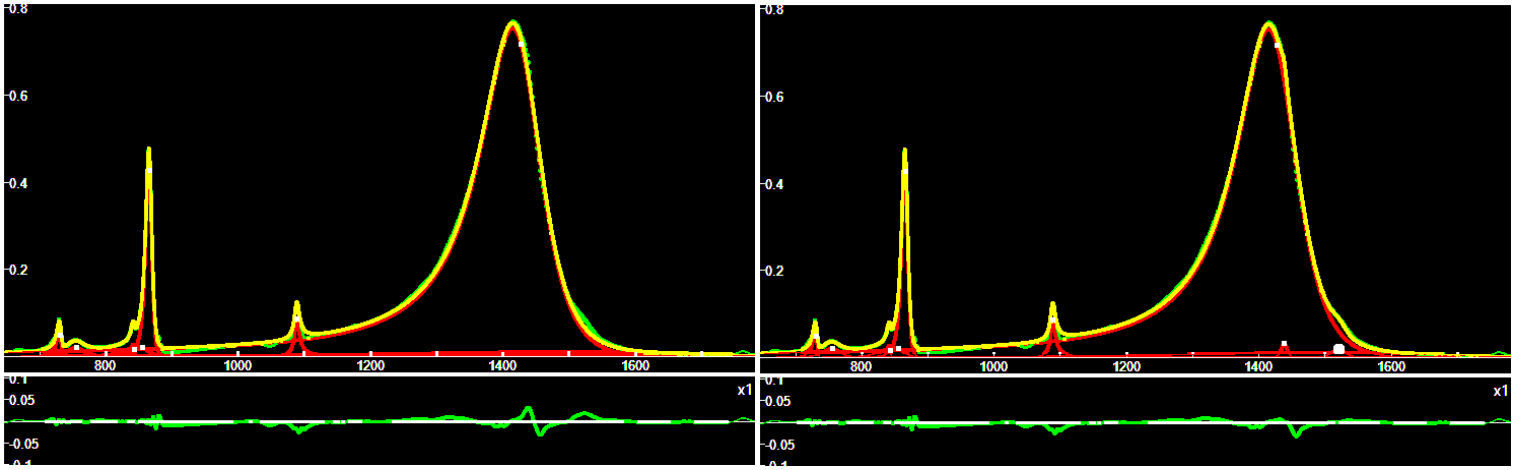

Fig.15: Deconvolution of bastnäsite-(Ce) R050409 ATR spectrum. On the left, one component is used for the main peak. On the right, two further very small components have been added. These two additional components seem being negligible.

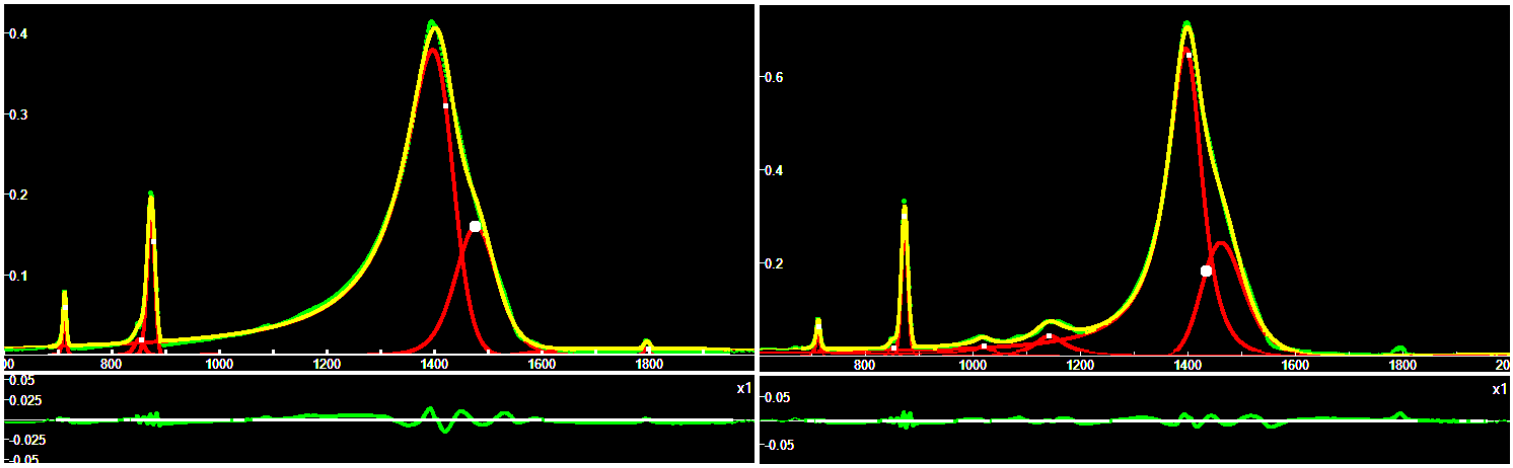

Fig. 16: Deconvolutions of calcite R040070 (on the left) and calcite R040170 (on the right) ATR spectra.

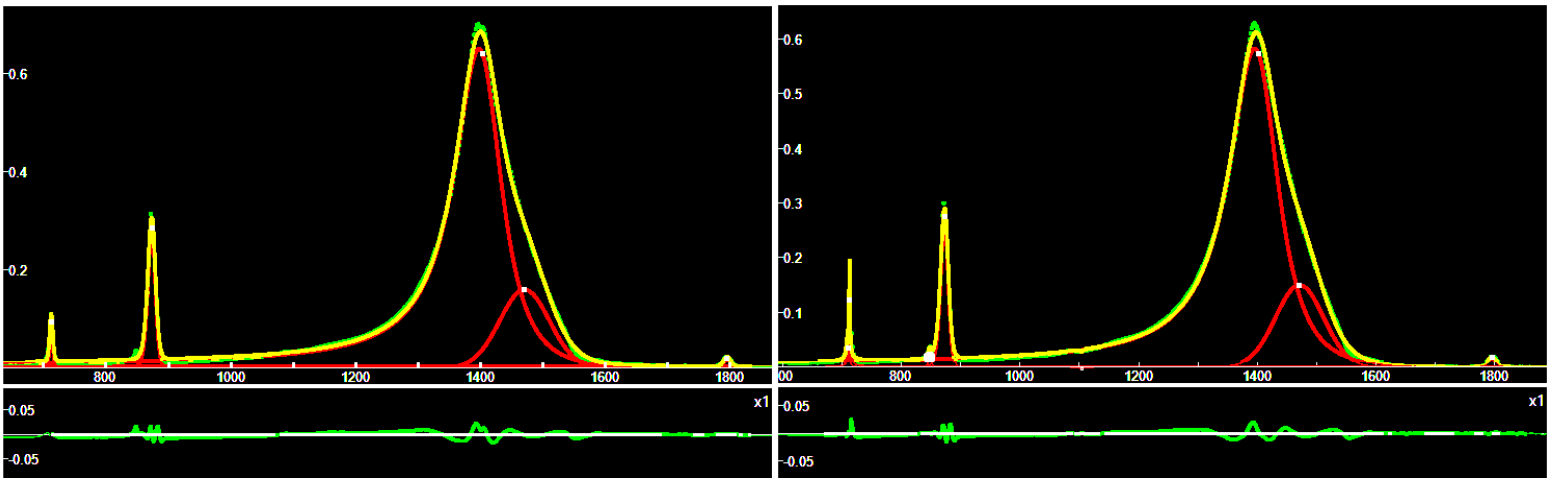

Fig.17: Deconvolutions of calcite R 050009 (on the left) and calcite R050048 (on the right) ATR spectra.

Calcite (Figures 16 and 17) is another interesting case where the "shoulder" is mentioned in literature.

Peaks positions in cm^{-1} ("sh" means "shoulder")

R040070	712		851	873		1398	1480	1796
R040170	713		851	873	1020 1144	1396	1465	1779
R050009	712		848	873	1090	1396	1481	1796
R050048	710	713	848	874		1396	1475	1795
Chukanov	712		847	876		1427	1470sh	1795

Further cases are given in the previous discussion about carbonate minerals.

In conclusion, we can tell that q-BWF functions are able to represent the general trend of the ATR spectra, without using a correction of the baseline. Regarding the additional q-BWF components, that we used to improve the fit, we can tell that, in the case of calcite, they are evidenced as shoulders also in literature.

Appendix A: q-Gaussians and q-BWF functions

The fitting of Raman spectra with q-Gaussian line shapes has been proposed for the first time in 2023 by A. C. Sparavigna. The q-Gaussian line shape is a function based on the Tsallis q-form of the exponential function (Tsallis, 1988). This exponential form is characterized by a q-parameter. When q is equal to 2, we have the Lorentzian function. If q is close to 1, we have a Gaussian function. For values of q between 1 and 2, we have a bell-shaped symmetric function with power-law wings ranging from Gaussian to Lorentzian tails. As shown on many occasions, the q-Gaussians are suitable for fitting Raman spectra (from examples proposed in SSRN to the SERS cases, for instance). However, we can define also an asymmetric function, turning the Breit-Wigner-Fano (BWF) into a q-BWF function (Sparavigna, 2023). Let us write the BWF as follow:

$$\mathrm{BWF}(x) = C\,\frac{\left[1-\xi\gamma^{1/2}(x-x_o)\right]^2}{\left[1+\gamma(x-x_o)^2\right]}$$

In the function given above, x_o represents the center of the line. When asymmetry parameter ξ is zero, BWF becomes a symmetric Lorentzian function. Note that the center of the line does not correspond to the position of the peak of the function. As in Sparavigna, 2023, we can define the q-BWF function in the following manner:

$$\text{q-BWF} = C\left[1 - \xi\gamma^{1/2}(q-1)^{1/2}(x-x_o)\right]^2[1+(q-1)\gamma(x-x_o)^2]^{1/(1-q)}$$

In fact, the Lorentzian function is substituted by a q-Gaussian function. The q-Gaussian is given as $f(x) = Ce_q(-\gamma x^2)$, where $e_q(.)$ is the q-exponential function and C a scale constant (Hanel et al., 2009). The q-exponential has expression: $e_q(u) = [1+(1-q)u]^{1/(1-q)}$. For spectroscopy, we write the q-Gaussian function with the center of the band at x_o:

$$q\text{-}Gaussian = Cexp_q(-\gamma(x-x_o)^2) = C\,[1+(q-1)\gamma(x-x_o)^2]^{1/(1-q)}.$$

We can apply q-Gaussian and q-BWF functions by means of Fityk software. In Fityk, a q-Gaussian function can be defined in the following manner:

define Qgau(height, center, hwhm, q=1.5) = height*(1+(q-1)*((x-center)/hwhm)^2)^(1/(1-q))

where q=1.5 is the initial guessed value of the q-parameter. Parameter hwhm is the half width at half maximum of the line. When q=2, the q-Gaussian is a Lorentzian function, that we can find defined in Fityk as:

Lorentzian(height, center, hwhm) = height/(1+((x-center)/hwhm)^2)

When q is close to 1, the q-Gaussian becomes a Gaussian function. The q-Breit-Wigner-Fano (q-BWF) can be defined as:

Qbreit(height, center, hwhm, q=1.5, xi=0.1) = (1-xi*(q-1)*(x-center)/hwhm)^2 * height*(1+(q-1)^0.5 *((x-center)/hwhm)^2)^(1/(1-q))

And the BWF can be defined as:

Breit(height, center, hwhm, xi=0.1) = (1-xi*(x-center)/hwhm)^2 * height/(1+((x-center)/hwhm)^2)

Using +xi instead of -xi does not change the fitting results in Fityk.
To have an asymmetric q-Gaussian, we could also consider a split-q-Gaussian function. For instance, in Fityk we find the split-Lorentzian:

SplitLorentzian(height, center, hwhm1=hwhm, hwhm2=hwhm) = x < center ? Lorentzian(height, center, hwhm1) : Lorentzian(height, center, hwhm2)

Therefore, we can define the split-q-Gaussian as:

Splitqgau(height, center, hwhm1=hwhm, hwhm2=hwhm, q1=1.5, q2=1.5) = x < center ? Qgau(height, center, hwhm1, q1) : Qgau(height, center, hwhm2, q2)

The two sides of the line shape have different q-parameters.

Appendix B: The principle of ATR (continued)

In Ramer and Lendl, 2006, we can find a history of ATR Spectroscopy. The authors start from quoting Newton and his Opticks, 1704, about the total reflection. Then, authors mention Elmer Hall, 1902, and the beginning of his *The penetration of totally reflected light into the rarer medium*. Hall wrote: "The fact that total reflection does not take place at the geometrical boundary of two media was discovered and experimentally investigated

by Newton. According to Newton the path of the ray during total reflection was a parabola, the vertex being within the rarer medium. The problem was both experimentally and theoretically studied by Fresnel, and more or less treated by Verdet, Young, Huygens, Biot, Babinet, Billet, Stokes, and others. The first reliable quantitative work was published by G. Quincke in 1866" (Hall, 1902).

Returning to the text by Ramer and Lendl: "Total reflection was, however, first used in the twentieth century for *absorption measurements* (Ramer and Lendl, mentioning Mirabella). In 1926, C.V. Raman, who went on to discover the Raman effect a few years later, reexamined the principles of total reflection. In the early 1930s, the principles of *ATR absorption measurements* were worked out by Taylor and Glover, Taylor and Durfee, and Taylor and King and employed to determine the birefringence of layers of organic acids" (see Ramer and Lendl and references therein). "In their work, the principles of ATR spectroscopy are laid out correctly and employed to measure absorption spectra, to study surface layers, and to determine refractive indices" (Ramer and Lendl, mentioning Mirabella). "The next major steps in the development of the ATR technique happened in quick succession in the late 1950s and the early 1960s. At the Fourth International Conference on Molecular Spectroscopy (Bologna, 1959), ~~Jacques~~ [Jacob] Fahrenfort of the Royal Dutch Shell Laboratories presented a paper on the ATR technique. In December of the same year [that is, 1959], at the Second International Conference on Semiconductor Surfaces (Maryland), Nicolas James Harrick of the Philips Laboratories suggested in a comment on a talk about 'Infrared Methods Applied to Surface Phenomena' (R.P. Eischens) to use ATR measurements to study molecules adsorbed on the surface" (Ramer and Lendl, mentioning Mirabella). "Harrick had been studying internal reflection and total internal reflection in semiconductors before" (Ramer and Lendl, mentioning Harrick, 1960). Let us stress, November 1959, Bologna Meeting and the work by Fahrenfort. "At this point, however, he [Harrick] presumably did know neither of the works of Taylor et al. nor of Fahrenfort's talk" (Ramer and Lendl, mentioning Mirabella). We have seen what Harrick wrote in his article of 1960. "Mirabella" means the reference as given by Ramer and Lendl: F.M. Mirabella, 'History of Internal Reflection Spectroscopy', in Internal Reflection Spectroscopy, ed. F.M. Mirabella, Marcel Dekker, Inc., New York, 1–16, Chapter 1, 1993. I was not able to find this specific edition.

It is interesting to read articles by Raman and by Taylor, to know how they addressed the problem of the Total Reflection. Raman, 1927, (not 1926 as given in Ramer and Lendl) considered the "Huygens' principle and the phenomena of total reflexion". In his paper, "the phenomena of total reflection are considered, de novo, from the standpoint of the principle of Huygens, no use whatever being made of the Fresnel formulae for reflection and refraction. Huygens' principle enables us to evaluate the disturbance appearing in the second medium when light is incident on the boundary between two media and is totally reflected into the first medium. The disturbance takes the form of a superficial wave moving parallel to the boundary. … . Finally, a method is described by which the distribution of intensity, state of polarisation, and direction of flow of energy in the superficial wave may be studied experimentally" (Raman, 1927). Raman is not mentioning the energy absorption.

In the discussions following the text of Raman's article, we find that T. Smith asked: "It is gratifying to find that the total reflection problem for a harmonic wave-train can be treated so thoroughly on the simple Huygenian principle. It would be still more satisfying to have a corresponding discussion in which events according to some of the modern quantum theories of light are considered; … Unlike the important question of phase, … the question whether the real light energy, that is the light quantum, penetrates the second medium does not appear to be yet answered. … ". Raman: "With regard to the question of energy it is clear that the elementary wavelets entering into the second medium attenuate each other's effects by interference so completely that the actual energy conveyed by them is an infinitesimal quantity". Raman continues mentioning formula (6) of his article. Below formula (6), it is written, regarding the "energy-flow in the superficial wave", that "it is entirely parallel to the surface, and thus the energy-flux across any element of area of the surface must be zero" (Raman, 1927). "Since there is no energy-flux across the boundary, it follows that the amplitudes of the incident and reflected waves must be equal." (Raman, 1927).

Regarding the studies by Taylor, in Taylor and Glover, we find investigation of refractive index. "In Part I four methods are described for measuring the refractive index of strongly absorbing liquids. The first two of these depend upon determination of the critical angle of reflection of *monochromatic light* at a glass-liquid interface.

In the third, *white light* was reflected at angles near the critical angle and was then allowed to enter a spectrograph. … In the fourth method the transmitted light was examined visually in a spectroscope. In Part II these methods have been applied to a saturated aqueous solution of potassium permanganate" (Taylor, & Glover, 1933). In Taylor and Durfee, 1933, "experiments are described which indicate by direct interferometric measurements the distance of penetration of light into the second medium at total reflection. ... A method of *multiple reflection* was devised … . The absorption coefficient and the refractive index of the liquid were measured in layers of the order of 10^{-3} cm thick and the values compared with the values deduced from the theoretical equations for the reflection coefficients. …". In Taylor and King, 1933, we can find an "extension of the second method for determining refractive indices of liquids in thin films, previously described in Part I of this series. …".

Then, let us add what was told by Blum and John, 2012. "For ATR the IR beam is passed through a crystal of a material with a high refractive index … This reflectance causes an evanescent wave that extends beyond the crystal's boundaries and penetrates the sample … IR radiation that is absorbed by the sample will cause the reflected evanescent wave to be attenuated. … Combination of ATR with FTIR leads to instruments using attenuated total reflectance – ATR-FTIR – allowing better sample-to-sample reproducibility and less user-to-user spectral variation. *The first application of ATR used with IR spectroscopy was presented by Harrick in 1960 and Fahrenfort in 1961*." If we are considering the ATR in IR spectroscopy, based on the energy absorption from evanescent field, Fahrenfort and Harrick must be mentioned as the people that independently proposed and developed the technique.

In Zhu et al., 1986, we find a review of the "frustrated total internal reflection". In this article, FTIR is the "frustrated total internal reflection", not the Fourier-transform infrared spectroscopy (FTIR), which is the technique used to obtain an infrared spectrum of absorption. As in Zhu and coworkers' article, let us have the light incident on the interface of two media. When n_1 index of medium 1 is greater than that the index n_2 of medium 2, total internal reflection can occur. "An intriguing phenomenon is the penetration of the wave (evanescent wave) or "disturbance" into the second medium when total reflection occurs" (Zhu et al., 1986). Newton, Fresnel, Verdet, Young, Huygens, Biot, Stokes, and Quincke were fascinated by the phenomenon. We can find references in Hall, 1902. "The theoretical exposition relied heavily on the slightly earlier (1900) presentation by Drude" (Zhu et al., 1986). To study the phenomenon, Hall used the common solution for the experimental set-up, adding a third medium, so that "the second medium is now a thin film with a thickness of the order of the wave-length of the light employed" between media 1 and 3. In this manner, the total reflection of light is thus "frustrated", "a term coined by Leurgans and Turner in 1947. If the second medium is absorbing, the term attenuated total reflection (ATR) has been used." (Zhu et al., 1986, and reference therein).

"Hall was perhaps unaware" of experiments by Bose, 1897. "In an ingenious experiment with two right angle prisms and one of the earliest generators of centimeter wave electromagnetic radiation, Bose examined the penetration of the waves by using the now canonical double-prism arrangement. His paper was communicated by Lord Rayleigh and appeared in the Proceeding of the Royal Society" (Zhu et al., 1986). Bose's experiment was repeated by Schaefer and Gross, Brady and coworkers, and Culshaw and Jones (see references in Zhu et al.). "Wood and Raman devoted some of their time to FTIR" (FTIR is the frustrated total internal reflection). Zhu and coworkers are referring to Raman, 1925, "On the Nature of the Disturbance in the Second Medium in Total Reflection". In this communication by Raman, we find told that in Raman's laboratory in Calcutta, B. N. Chuckerbutti, in 1920, investigated an optical phenomenon: "he let a pencil of highly monochromatic light pass into and, through a glass prism in such manner that it emerged almost grazing the surface of the prism by which it made its exit. Diffraction patterns are seen through the observing telescope that receives the emergent beam ... these patterns continue to appear even when the angle, at which the ray in the glass strikes the final surface, is larger than the critical angle. … There is thus final evidence that light does penetrate into the second medium when the angle of incidence is larger than the critical angle".

"Advances in the theoretical understanding beyond the work of Hall were made by Eichenwald, Foersterling, and Arzelies, who studied the energy flow and arrived at the notion of exponentially decaying evanescent wave. The effect of a finite cross section for the incident beam, rather than an infinite plane wave, was discussed by Picht" (Zhu et al., 1986, and references therein). "Despite these theoretical advances, the

discovery of the Goos-Hänchen shift in 1947 caused some controversy" (Zhu et al., 1986). "This effect [Goos-Hänchen shift] continues to be a topic of scientific research" (Wikipedia).

"The discovery of barrier penetration in quantum mechanics brought the insight that it was a phenomenon rather analogous to FTIR. Hence the name "optical tunneling" for FTIR which is used fairly often in quantum-mechanics text. It has, in fact, become quite popular to quote FTIR as an illustration of quantum mechanical tunnelling" (Zhu et al., and references therein; see experiment in the physlab.org/class-demo/optical-tunneling/).

In Sprokel and Swalen, 1997, it is told that the attenuated total reflection (ATR) "differs from other, perhaps better-known procedures, such as ellipsometry and reflectometry, in that ATR probes the sample with an evanescent wave rather than a collimated beam of light". When "an evanescent wave can be made to interact with material in its field ", "energy can be transported. Then the reflectivity will be less than unity and hence the term attenuated total reflectivity". "Evanescent waves can also be generated by gratings, and historically the use of gratings preceded that of prisms; however, the prism technique is simpler by far. The prism geometry has been employed in internal reflection spectroscopy (IRS) for many years. The light enters a prism, and the sample is pressed to its base. It is well detailed by Harrick" (Sprokel and Swalen, mentioning Harrick, 1967).

We have seen that it was at the meeting in Bologna, 1959, that Fahrenfort proposed the technique of ATR for infrared spectroscopy, instead of the transmission technique. And that Harrick published in 1960, the multireflection approach. But in Sprokel and Swalen we find told that ATR encompasses "widely differing phenomena as plasmon waves on metal surfaces and certain organic dyes, guided modes in dielectric films, and surface waves on diffraction gratings", and that "ATR evolved as a technique in 1968 mostly through the work of Otto in Munich and Raether and Kretschmann in Hamburg" (Sprokel & Swalen, and .references therein). The articles by Otto and Kretschmann and Raether are regarding surface plasmons. "Although surface-plasmon waves were known since the work of Sommerfeld", 1909, "they received little attention in optics until the work of Fano in 1941" (Sprokel & Swalen, and references therein). "Fano recognized that surface electromagnetic (EM) waves are evanescent waves with wave vectors larger than that of the incident beam"; Sprokel and Swalen continue with further references about the plasmon waves, and optics of Langmuir-Blodgett films, integrated optics applied to Raman scattering, and the optics of organic thin films.

References

1. Baxter, B. H., & Puttnam, N. A. (1965). Multi-reflexion Attenuated Total Reflectance Infra-red Spectroscopy. Nature, 207(4994), 288-288.
2. Bicchieri, M., Nardone, M., Russo, P.A., Sodo, A., Corsi, M., Cristoforetti, G., Palleschi, V., Salvetti, A., & Tognoni, E. (2001). Characterization of azurite and lazurite based pigments by laser induced breakdown spectroscopy and micro-Raman spectroscopy. Spectrochimica Acta Part B: Atomic Spectroscopy, 56(6), pp.915-922.
3. Blum, M. M., & John, H. (2012). Historical perspective and modern applications of attenuated total reflectance–Fourier transform infrared spectroscopy (ATR-FTIR). Drug testing and analysis, 4(3-4), 298-302.
4. Bose, J. C. (1898). On the influence of the thickness of air-space on total reflection of electric radiation. Proceedings of the Royal Society of London, 62(379-387), 300-310.
5. Chukanov, N.V. (2014). IR Spectra of Minerals and Reference Samples Data. Springer Geochemistry/Mineralogy. Springer, Dordrecht. doi:10.1007/978-94-007-7128-4_2
6. Deane, A. M., Richards, E. W. T., & Stephen, I. G. (1966). Bond orientations in uranyl nitrate hexahydrate using attenuated total reflection. Spectrochimica Acta, 22(7), 1253-1260.
7. Devlin, J. P., Pollard, G., & Frech, R. (1970). ATR infrared spectra of uniaxial nitrate crystals. The Journal of Chemical Physics, 53(11), 4147-4151.
8. D'Ippolito, V., Andreozzi, G. B., Bersani, D., & Lottici, P. P. (2015). Raman fingerprint of chromate, aluminate and ferrite spinels. Journal of Raman Spectroscopy, 46(12), 1255-1264
9. Ekgasit, S., & Padermshoke, A. (2001). Optical contact in ATR/FT-IR spectroscopy. Applied spectroscopy, 55(10), 1352-1359.

10. Fahrenfort, J. (1961). Attenuated total reflection: A new principle for the production of useful infrared reflection spectra of organic compounds. Spectrochimica Acta, 17(7), 698-709.
11. Fahrenfort, J., & Visser, W. M. (1962). On the determination of optical constants in the infrared by attenuated total reflection. Spectrochimica Acta, 18(9), 1103-1116.
12. Fano, U. (1941). The theory of anomalous diffraction gratings and of quasi-stationary waves on metallic surfaces (Sommerfeld's waves). JOSA, 31(3), 213-222.
13. Fenske, M. R., Braun, W. G., Wiegand, R. V., Quiggle, D., McCormick, R., & Rank, D. H. (1947). Raman spectra of hydrocarbons. Analytical Chemistry, 19(10), 700-765.
14. Forbes, R. J. (1955). Studies in Ancient Technology, Volume 1. Brill Archive.
15. Frost, R. L., Martens, W. N., Rintoul, L., Mahmutagic, E., & Kloprogge, J. T. (2002). Raman spectroscopic study of azurite and malachite at 298 and 77 K. Journal of Raman Spectroscopy, 33(4), 252-259.
16. Graf, R.T., Koenig, J.L., Ishida, H. (1987). Introduction to Optics and Infrared Spectroscopic Techniques. In: Ishida, H. (eds) Fourier Transform Infrared Characterization of Polymers. Polymer Science and Technology, vol 36. Springer, Boston, MA. https://doi.org/10.1007/978-1-4684-7776-4_1
17. Hall, E. E. (1902). The penetration of totally reflected light into the rarer medium. Physical Review (Series I), 15(2), 73.
18. Han, K., Nam, J.Y., Ji, J.E., Kang, D., Lee, H., Baek, N., Song, Y. and Yang, I.S., 2016. Existence of nanoparticles in azurite and malachite pigments–Raman spectroscopy and X-ray diffraction studies. Dyes and pigments, 133, pp.232-237.
19. Hanel, R., Thurner, S., & Tsallis, C. (2009). Limit distributions of scale-invariant probabilistic models of correlated random variables with the q-Gaussian as an explicit example. The European Physical Journal B, 72(2), 263.
20. Hansen, W. N., & Horton, J. A. (1964). Spectrometer Cells for Single and Multiple Internal Reflection Studies in Ultraviolet, Visible, Near Infrared, and Infrared Spectral Regions. Analytical Chemistry, 36(4), 783-787.
21. Harrick, N. J. (1960). Study of physics and chemistry of surfaces from frustrated total internal reflections. Physical Review Letters, 4(5), 224.
22. Harrick, N. J. (1964). Multiple Reflection Cells for Internal Reflection Spectrometry. Analytical Chemistry, 36(1), 188-191.
23. Harrick, N. J. (1967). Internal Reflection Spectroscopy, Wiley, New York.
24. Ivanovski, V., Mayerhöfer, T. G., & Popp, J. (2009). Employing polyethylene as contacting agent between ATR-crystals and solid samples with hard surfaces. Journal of Molecular Structure, 924, 571-576.
25. Kendix, E. L. (2009). Transmission and Reflection (ATR) Far-Infrared Spectroscopy Applied in the Analysis of Cultural Heritage Materials. Ph.D. Thesis, Alma Mater Studiorum Università di Bologna, Bologna, Italy.
26. Kendix, E. L., Prati, S., Joseph, E., Sciutto, G., & Mazzeo, R. (2009). ATR and transmission analysis of pigments by means of far infrared spectroscopy. Analytical and bioanalytical chemistry, 394, 1023-1032.
27. Kretschmann, E., & Raether, H. (1968). Radiative decay of non radiative surface plasmons excited by light. Zeitschrift für Naturforschung A, 23(12), 2135-2136.
28. Kuehn, J. W. (2014, December). Raman and photoluminescence spectroscopy in gem identification. In The 4th International Gem & Jewelry Conference (GIT 2014).
29. Lafuente, B., Downs, R. T., Yang, H., & Stone, N. (2015). 1. The power of databases: The RRUFF project. In Highlights in mineralogical crystallography (pp. 1-30). De Gruyter (O).
30. Makreski, P., & Jovanovski, G. (2003). Minerals from Macedonia. IX. Discrimination between some orthorhombic carbonates by FTIR spectroscopy. Bulletin of the Chemists and Technologists of Macedonia, 22, 25–32 (2003).

31. Mendoza-Galván, A., Méndez-Lara, J. G., Mauricio-Sánchez, R. A., Järrendahl, K., & Arwin, H. (2021). Effective absorption coefficient and effective thickness in attenuated total reflection spectroscopy. Optics Letters, 46(4), 872-875.
32. Mosier-Boss, P. A., Lieberman, S. H., & Newbery, R. (1995). Fluorescence rejection in Raman spectroscopy by shifted-spectra, edge detection, and FFT filtering techniques. Applied Spectroscopy, 49(5), 630-638.
33. Otto, A. (1968). Excitation of nonradiative surface plasma waves in silver by the method of frustrated total reflection. Zeitschrift für Physik A Hadrons and nuclei, 216(4), 398-410.
34. Paschotta, R. (2024). Optical Contact Bonding. In the RP Photonics Encyclopedia, retrieved 2024-10-08, https://doi.org/10.61835/9yp
35. Piro, O. E., Castellano, E. E., & Gonzalez, S. R. (1988). Attenuated total-reflectance spectra of strongly absorbing anisotropic single crystals: Trigonal α-quartz. Physical Review B, 38(12), 8437.
36. Prasad, P. S. R., Krishna Chaitanya, V., Shiva Prasad, K., & Narayana Rao, D. (2005). Direct formation of the γ-CaSO4 phase in dehydration process of gypsum: In situ FTIR study. American Mineralogist, 90(4), 672-678.
37. Raman, C. V. (1925). On the nature of the disturbance in the second medium in total reflection. Philosophical Magazine, 1925, Vol.50, p812-815
38. Raman, C. V. (1927). Huygens' principle and the phenomena of total reflexion. Transactions of the Optical Society (London), 28(3), 149. Link.
39. Ramer, G., & Lendl, B. (2006). Attenuated Total Reflection Fourier Transform Infrared Spectroscopy. Encyclopedia of analytical chemistry: applications, theory and instrumentation.
40. Sparavigna, A. C. (2024). The Raman Fingerprints of Quartz, Albite and Calcite (October 10, 2023). Available at SSRN: https://ssrn.com/abstract=4594641 or http://dx.doi.org/10.2139/ssrn.4594641
41. Sparavigna, A. C. (2023). q-Gaussian Tsallis Line Shapes and Raman Spectral Bands. Int. J. Sciences, 12(3), 27-40.
42. Sparavigna, A. C. (2023). Asymmetric q-Gaussian functions generalizing the Breit-Wigner-Fano functions. Zenodo. https://doi.org/10.5281/zenodo.8356165
43. Sparavigna, A. C. (2024). Raman Spectroscopy of Siderite with q-Gaussian and split-q-Gaussian Analyses. International Journal of Sciences, 13(02), 8-21.
44. Sparavigna, A. C. (2024). Hydroxyl-Stretching Region in the Raman Broad Scans on Minerals of the Vivianite Group (Vivianite, Baricite, Bobierrite, Annabergite, Erythrite). Int. J. Sciences, 13(08), 23-36.
45. Sparavigna, A. C. (2024). Water in zeolites of natrolite group and its OH-stretching region in Raman spectroscopy. ChemRxiv. https://doi.org/10.26434/chemrxiv-2024-wdv4b
46. Sparavigna, A. C. (2024). q-BWF functions to deconvolute the attenuated total reflectance infrared spectra of the barite-group minerals. ChemRxiv, https://doi.org/10.26434/chemrxiv-2024-9x1jz
47. Sparavigna, A. C. (2024). Attenuated Total Reflectance Infrared Spectra of Carbonate Minerals, Deconvoluted by Means of q-BWF Functions. International Journal of Sciences, 13(09), 76-83. http://dx.doi.org/10.18483/ijSci.2803
48. Sparavigna, A. C. (2024). Gypsum Crystallization Water: Comparing a Laser Excited Raman Spectrum with a Mercury Resonance Radiation Excited Spectrum (Rasetti Technique). International Journal of Sciences, 13(09), 42-49. http://dx.doi.org/10.18483/ijSci.2798
49. Sprokel, G. J., & Swalen, J. D. (1997). The attenuated total reflection method. In Handbook of optical constants of solids (pp. 75-95). Academic Press.
50. Subramanian, A., & Rodriguez-Saona, L. (2009). Chapter 7-Fourier Transform Infrared (FTIR) Spectroscopy, in Infrared Spectroscopy for Food Quality Analysis and Control, D. Sun, Ed.
51. Taylor, A. M., & Glover, A. M. (1933). Studies in refractive index. I and II. JOSA, 23(6), 206-215.
52. Taylor, A. M., & Durfee, D. A. (1933). Studies in Refractive Index. III1. JOSA, 23(8), 263-269.
53. Taylor, A. M., & King, A. (1933). Studies in Refractive Index. Part IV. JOSA, 23(9), 308-312.
54. Tsallis, C. (1988). Possible generalization of Boltzmann-Gibbs statistics. Journal of statistical physics, 52, 479-487.

55. Vahur, S., Teearu, A., Peets, P., Joosu, L., & Leito, I. (2016). ATR-FT-IR spectral collection of conservation materials in the extended region of 4000-80 cm–1. Analytical and Bioanalytical Chemistry, 408, 3373-3379.
56. Wang, C., Ren, L. A., Walters, J. B., Zhang, L., & Tao, R. (2023). In situ Raman vibrational spectra of siderite (FeCO3) and rhodochrosite (MnCO3) up to 47 GPa and 1100 K. American Mineralogist, 108(2), 312-325.
57. Wojdyr, M. (2010). Fityk: a general-purpose peak fitting program. Journal of applied crystallography, 43(5), 1126-1128.
58. Zhu, S., Yu, A. W., Hawley, D., & Roy, R. (1986). Frustrated total internal reflection: A demonstration and review. American Journal of Physics, 54(7), 601-607.
59. Zhu, Y., Li, Y., Ding, H., Lu, A., Li, Y., & Wang, C. (2021). Multifactor-controlled mid-infrared spectral and emission characteristic of carbonate minerals (MCO 3, M= Mg, Ca, Mn, Fe). Physics and Chemistry of Minerals, 48, 1-12.
60. Zolotarev, V. M. (2000). Development of methods and techniques for attenuated total reflection (ATR) spectroscopy. Journal of Optical Technology, 67(4), 309.